COMPUTATION OF SEISMIC DEFORMATIONS OF

OFFSHORE SLOPES ON CLAYS AND SANDS

by

SARATH BANDARA SAMARASINGHE ABAYAKOON

B.Sc(Eng.Hons.), University Of Peradeniya, Sri Lanka, 1979

A THESIS SUBMITTED IN PARTIAL FULFILMENT OF

THE REQUIREMENTS FOR THE DEGREE OF

MASTER OF APPLIED SCIENCE

in

THE FACULTY OF GRADUATE STUDIES

Department Of Civil Engineering

We accept this thesis as conforming

to the required standard

THE UNIVERSITY OF BRITISH COLUMBIA

July 1983

In presenting this thesis in partial fulfilment of the
requirements for an advanced degree at the University
of British Columbia, I agree that the Library shall make
it freely available for reference and study. I further
agree that permission for extensive copying of this thesis
for scholarly purposes may be granted by the head of my
department or by his or her representatives. It is
understood that copying or publication of this thesis
for financial gain shall not be allowed without my written
permission.

Department of ___*Civil Engineering*___

The University of British Columbia
1956 Main Mall
Vancouver, Canada
V6T 1Y3

Date ___*28ᵗʰ July 1983*___

A B S T R A C T

A critical review of presently available methods for analysing offshore slopes under earthquake loading is presented herein. New methods of analysis, based on both rigid body mechanics and flexible non-linear constitutive equations are presented and discussed.

In rigid body type analyses, a yield acceleration is calculated and displacements are evaluated by double integrating the accelerations in excess of the yield. This type of analyses takes neither the amplification or deamplification of the acceleration through the deposit nor the continuous relative displacements throughout the soil mass into account. Furthermore, when the slope is submerged, buoyant and pore water pressures must be included in the analysis.

Flexible, non-linear computer models are available to overcome the drawbacks in rigid body methods. Two recently developed non-linear models, DONAL-2 and DCHARMS, are described. Rigid body analysis methods are compared with non-linear models by applying them to calculate displacements of example slopes.

On the basis of the results of these comparisons, it was concluded that the displacements of offshore slopes should be computed by non-linear analyses.

TABLE OF CONTENTS

LIST OF TABLES

LIST OF FIGURES

Dedication

To My late Father

ACKNOWLEDGEMENT

CHAPTER 1

INTRODUCTION.

After the discovery of oil at lake Maracaibo, Venezula, modern development of offshore construction started in this area in the 1920s. However,the role of the geotechnical engineer in the offshore construction industry was overlooked until the 1960s, when oil drilling was started in the deep waters of the gulf of Mexico. The work, which has to be carried out by the geotechnical engineer is basically twofold. First, the safety of the structure has to be considered with respect to its foundations. This includes the responsibility for soil investigations, stability calculations for the platform, and the foundation design. Secondly, stability of the seafloor is of major importance for offshore structures such as gravity structures and pipelines.

Stability of the seafloor can be disturbed either by wave action or by the inertia forces produced by an earthquake. Residual pore water pressures might build up in some soils due

to the cyclic shear stresses induced in the seabed by these actions (Finn et al.,1976). This might lead to loss of strength and consequently to the occurence of seafloor slides which in turn may cause a severe loading condition on the offshore structures. The occurences of seafloor instability due to wave action has been reported and extensively studied. However, as there are differences between seismic loading and wave loading, seafloor stability under earthquakes has to be analysed separately. It is to this problem that this thesis is directed.

Earthquakes originate at a fault zone with a sudden release of strains, which are accumulated over the years. Such a strain release will be propagated towards the earth's surface through the earth's crust in a somewhat elastic manner. Since the early forties, several researchers and engineers have been working on the problem of earthquakes. The damage to, and the response of steel and concrete structures under the earthquake forces have been studied thoroughly during this period. Extension of this study to the area of soil mechanics has been accomplished and considerable advances have been made in the past twenty-five years. Satisfactory methods of designing large earth structures such as dams and embankments are available as a result of such studies.

Analysis of offshore slopes under earthquake forces is a rather new problem. Since it is extremely difficult, if not impossible, to redesign a underwater slope to meet some design requirements, this is essentialy a stability analysis

rather than a design assignment. One should be able to calculate the displacements of an offshore slope due to the action of a design earthquake. The design engineer for the offshore construction company can then take the necessary precautionary measures against the adverse effects of such movements.

Tackling of this problem can be initiated by carefully studing the available stability analysis methods for slopes ashore. Permanent deformations in ground slopes under cyclic loading can be calculated by various means. The state of the art for analysing such deformations was recently assessed in a report on earthquake engineering research by the National Research Council of the United States (Finn, 1983; USNRC, 1982):

> "Many problems in soil mechanics, such as safety studies of earth dams, require that the possible permanent deformations that would be produced by earthquake shaking of prescribed intensity and duration be evaluated. Where failure develops along well defined failure planes, relatively simple elastoplastic may suffice to calculate displacements. However, if the permanent deformations are distributed throughout the soil, the problem is much more complex, and practical, reliable methods are not available. Future progress will depend on development of suitable plasticity models for soil undergoing repetitive loading. This

is currently an inportant area of research."

It is clear from this that although there are a number of methods available for analysing the problem, practicality and reliability of those methods is still in question.

Two years ago, the Soil Dynamics group of the University of British Columbia was asked by ERTEC Western Incorporated, Long Beach, California, to develop a method to calculate deformations in offshore slopes under earthquakes. This request was made because of the involvement of the above mentioned consulting company in designing offshore structures in the Mediterranean sea, off the coast of Spain. As a result, the true non-linear computer programme DONAL-2 (Iai and Finn, 1982) was developed by the soil dynamics group. The work reported in this thesis is a continued study of the same problem.

As sampling and in-situ testings are extremely difficult to carry out in the rough waters of most offshore sites, evaluation of parameters to use in a complex analysis procedure is troublesome. Even if sampling is done, it will be severely disturbed and only the residual parameters could be evaluated by subsequent laboratory testing. Hence, in the present study, attention was focused on the modification of more simple methods.

Some of the presently available rigid body motion

methods were considered for offshore slope applications. In all the methods, a yield acceleration, i.e. the acceleration at which slippage will begin to occur and at which deformations develop, will be calculated. By integrating the effective acceleration, in excess of the yield acceleration, as a function of time, velocities and ultimately the displacements of the sliding mass could be evaluated. These methods were then compared with DONAL-2 programme, by the use of examples. Finally, a newly developed computer programme, DCHARMS (Moriwaki et al., 1982), was also compared with DONAL-2. Advantages, limitations and the use, of every method is critically analysed.

CHAPTER 2

STABILITY ANALYSIS METHODS AVAILABLE FOR ASSESSING THE

BEHAVIOUR OF SLOPES UNDER EARTHQUAKE LOADING.

2.1 Introduction.

Before going on to the problem of offshore slopes, it is necessary to investigate the presently available methods of earthquake stability analysis for slopes on shore. Depending on their relative advantages and disadvantages, and the soil parameters and test data required, it is then possible to determine whether they can be modified for the analysis of offshore slopes under dynamic loading.

The usual factor of safety approach for static analysis of ground slopes was originally used for dynamic analysis as well, as discussed in Section 2.2, through a pseudo-static procedure.

It was later realized (Newmark, 1965; Seed, 1966) that the seismic performance of soil structures should be evaluated in terms of deformation rather than in terms of factor of safety. Section 2.3 describes methods for calculating

downslope displacements of earth slopes under dynamic loading. In these methods, soil mass was either considered as a rigid body or as a deformable body. Advantages and limitations of such methods are also discussed in this section.

Section 2.4 deals with the two non-linear computer programmes presently available to calculate displacements in an offshore slope under seismic loading. A description of the programmes is given with their relative merits and drawbacks.

2.2 Factor of Safety Approach.

The usual concept of the factor of safety has been used to assess the stability of slopes on land, under static forces as well as dynamic forces. In almost all the conventional methods, the factor of safety is defined as the ratio of shear strength to the shear stress induced. In addition, the same factor of safety is used for the cohesion and for the tangent of internal friction in most of the methods. Furthermore, the same 'F' is assumed at every point on the potential failure surface. In usual slope stability analyses, a calculated factor of safety less than unity implies a complete failure.

In the so called pseudo-static method of dynamic analysis, the factor of safety is calculated by introducing the inertia force as a static horizontal force of appropriate magnitude. This force is expressed as the product of a seismic

coefficient 'k' and the weight 'W' of the sliding mass. The seismic coefficient is calculated by one of three methods (Seed and Martin,1966).

1.Use of Emperical Values.

In North American practice, the inertia force is calculated by multiplying the weight of sliding mass by a coefficient ranging from 0.05-0.15. In Japan, however, the seismic coefficient is chosen from a range of 0.12-0.25, depending on the location of the slope, the type of foundation etc.. The Russian code, considers a variation of seismic coefficient with depth (Ambraseys,1960). In spite of the popular use of these values during the past, there is no reasonable basis for choosing a coefficient of this order of magnitude.

2. Rigid Body Response Analysis.

Seismic coefficient can also be calculated by a rigid body type analysis. If a slope is behaving as a rigid body, inertia force produced by an earthquake will be equal to the mass times the ground acceleration. Design seismic coefficients for slopes on shore were hence chosen as the maximum ground acceleration recorded during the earthquake. However, this method suffers from two main disadvantages.

a) Maximum ground acceleration developed for only a short period of time. Hence, a large amount of conservatism will be built into the calculated Factor of Safety. On the other hand, although there is a series of accelerations and corresponding inertia forces during an earthquake, the combined effect of these should not necessarily be equal to the effect produced by the inertia force generated by the maximum acceleration, acting as a static force.

b) Applicability of rigid body motion is limited to stiff and/or small slopes with small slope angles. There is hardly any equivalence between the response of the slopes of large dams subjected to dynamic loading and the rigid body response, as revealed by field tests.

3. Elastic Response Analysis.

Methods of elastic response analysis were developed to overcome the disadvantages in previously discussed methods, in calculating seismic coefficients. In most of these methods, slope was assumed to be made up of thin horizontal slices, which were connected by linearly elastic springs and viscous damping devices. Response of such a system to an earthquake motion is analysed by inputting the seismic loading at the base. By this method, one can

incorporate different seismic coefficients at different levels of the earth structure, and hence different displacements. Analyses of this type were carried out using various assumptions of shear modulus variation and the mode of failure, by several investigators (Mononobe et al.,1936; Hatanaka,1955; Ambraseys,1960; Rashid,1961; Krishna,1962). Ambraseys' methods resulted in a seismic coefficient varying with the depth of the soil structure. The analysis was further extended by Byrne (1969), with the inclusion of plastic behaviour, for large scale vibrations. Yet, he did not use the model to calculate seismic coefficients as he was only interested in displacements.

The elastic response analysis methods, however, assume that the ground motion is controlled only by shearing action developed between horizontal slices. Furthermore, one has to be very careful in selecting the equivalant damping coefficients and modulus values as they are very much affected by various factors.

As explained before, empirical methods have little or no rational basis for selecting a seismic coefficient. Moreover, whether the coefficient is determined by rigid body, viscoelastic or elastic-viscoplastic analysis, the designer should accept that, any deformation, whether small or large,

calculated by a pseudo-static type analysis, constitutes a failure (Seed,1967). This is a very conservative approach to the problem. In addition, in comparing the different methods of calculating seismic coefficients, a wide range of choice is seen for the selection of a proper value for the design, reflecting the uncertainity of engineers regarding the method.

2.3 Displacement Approach.

After Newmark's classic paper (1965) on "Effects of earthquakes on Dams and Embankments", several researchers in the world are continuing studies to find better methods of analysing the earthquake stability of slopes. Newmark (1965) and Seed (1966) have both criticized the use of the usual concept of a factor of safety on shear strength to assess the performance of an earth slope during strong earthquakes. A factor of safety less than unity does not necessarily mean a failure in a dynamic analysis as the inertia forces are developed only for a small period of time. Permenant deformations will occur once the factor of safety drops below one, but these movements will be arrested when the magnitude of the acceleration is decreased or is reversed. Hence, the performance of the slope should be measured in terms of the relative displacements that the soil mass may undergo during and after the earthquake. The total displacement can be calculated by adding up the small deformations that occur whenever the factor of safety goes below unity. Depending on

the magnitude of the movement, subsequent precautions can be
carried out. It is to be noted at this stage that there will
not be any movement after the earthquake, unless the strength
of the soil has dropped below the original in-situ shear
stresses in the slope, provided creep effects and consolidation
in the post cycle period are neglected.

Methods of displacement calculations in a ground
slope under earthquake loading may be classified into two broad
categories. In the first category, soil mass is considered as a
rigid body and in the second, it is considered as a deformable
body.

2.3.1. Rigid Body type analysis.

Newmark (1965), introduced rigid body approach by
considering the motion of a block on a horizontal plane (Fig
2.1). If the motion of the plane is designated by $y(t)$, and if
the true displacement of the block is x, the motion of the
block relative to the plane is given by,

$$u = x - y \qquad (2.1)$$

Assuming that the shearing resistance of the plane is
equal to kW where W is the weight of the block, it is
equivalent to an acceleration of the ground of magnitude kg.
Now, if an acceleration pulse of magnitude Ag (Fig. 2.2), acts
on the base, the resulting acceleration,
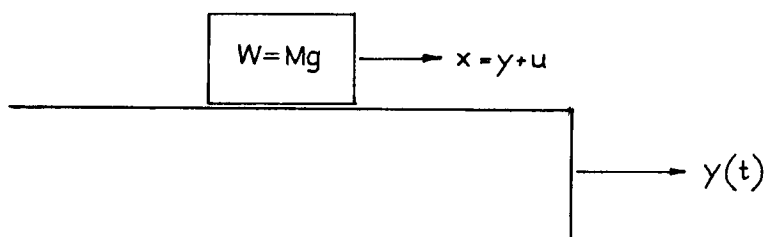
Fig.2.1   Rigid Block on a Moving Support
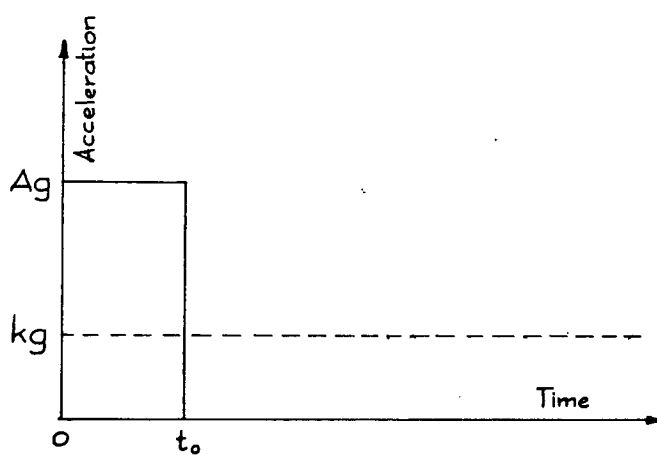
Fig.2.2   Rectangular Block Acceleration Pulse

$$\ddot{u} = (A - k) g \qquad (2.2)$$

and the velocity, $\qquad \dot{u} = (A - k) gt \quad , t < t_0$

and $\qquad \dot{u} = Agt_0 - kgt \qquad , t > t_0$ $\qquad (2.3)$

The motion will be stopped when $\dot{u} = 0$, i.e. ,when $t_m = At_0 /k$

The displacement relative to the ground during the period t_m can be calculated by integrating the velocity.

$$u = \int_0^{t_0}(A - k)gt \, dt + \int_{t_0}^{t_m}(Agt_0 - kgt) \, dt$$

$$= \frac{V^2}{2gk} \left(1 - \frac{k}{A} \right) \qquad \text{where} \quad V = Agt_0 \qquad (2.4)$$

Newmark considers the preceeding approach to be a conservative one as the actual situation corresponds to a number of pulses in random order, some positive and some negative. However, as the ground comes to rest at the end of the earthquake motion, area under the acceleration curve should be zero.

By extending the above result, one can calculate the displacement under a group of pulses when the resistance in either direction of possible motion is the same. If these resistances are different, a different analysis has to be carried out. A horizontal plane having such a differential resistance is equivalant to a sloping surface of uniform resistance (Fig. 2.3). If the limiting friction force per unit normal force is tan ϕ',

for motion down the slope,

$$k_d = \text{Sin } i \left(\frac{\tan \phi'}{\tan i} - 1 \right) \qquad (2.5)$$

and for motion up the slope,

$$k_u = \text{Sin } i \left(\frac{\tan \phi'}{\tan i} + 1 \right) \qquad (2.6)$$

where, k_d and k_u are the yield accelerations downslope and up slope respectively. In the problems usually encountered in practice, k_u will be sufficiently larger than k_d , so that the motion up slope can be neglected. In other words, an infinite yield acceleration is assumed for motion up the slope.

Newmark presented his results in graphical form giving the relationship between standardized maximum displacement and k / A, the ratio of maximum resistance coefficient to the maximum earthquake acceleration. For these calculations, he selected four earthquakes with maximum ground accelerations varying from 0.17 to 0.32, and all four earthquakes were normalized to a maximum acceleration of 0.5g and a maximum ground velocity of 30 in/sec. The comparison between model tests and the theory was satisfactory for symmetrical resistance, for the values of k/A greater than 0.1. On the contrary, the results did not tally for the unsymmetrical case.

Seed and Goodman (1964), used the rigid body approach with a horizontal ground acceleration instead of the acceleration parallel to the surface, used by Newmark (Fig. 2.4).

yielding,

$$k_{horiz} = \tan (\phi - i) \qquad (2.7)$$

They have performed model tests to verify the accuracy of this expression and introduced a shear strength intercept, which has a profound effect on yield accelerations of small embankments. The effect of this is to shift the sliding surface down and to create a resisting wedge at the toe of an embankment with a finite length. These results lead to a modification of the expression for yield acceleration to,

$$k_{horiz} = \tan (\phi_{eq} - i) \qquad (2.8)$$

where, $\phi_{eq} = \phi + \phi_{sl}$ includes the effects of the shear strength intercept.

In calculating the displacements of a finite slope by the use of above expression, Goodman and Seed (1966) assumed a reduction in shear strength with increasing displacement (Fig. 2.5). At this stage it is worthwhile to note that the friction angle ϕ is also a function of the normal force (Taylor, 1948). As the normal force on the slope is again a function of the acceleration, analysis will be more complicated if one is to
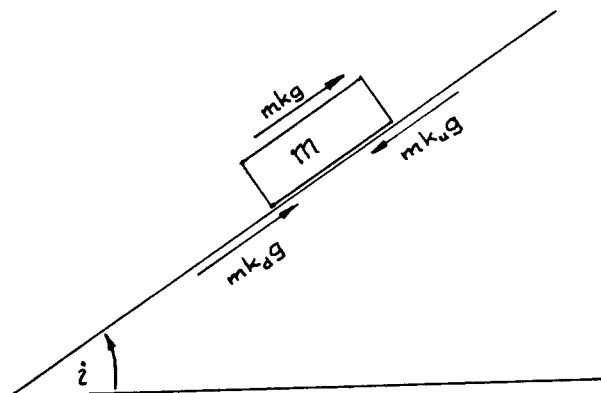
Fig.2.3   Unsymmetrical Yield Acceleration
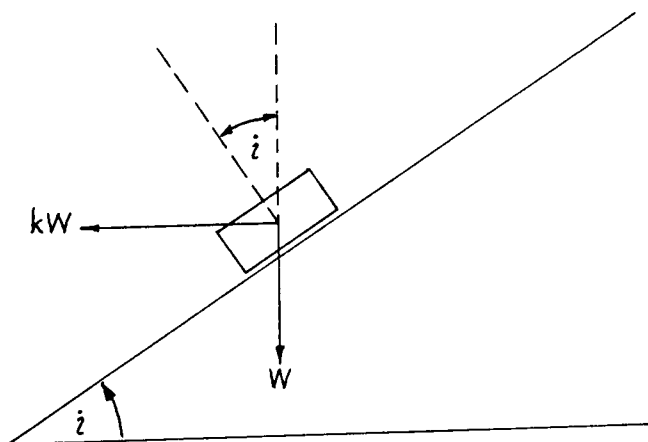
Fig.2.4   Horizontal Acceleration (Seed and Goodman, 1964)
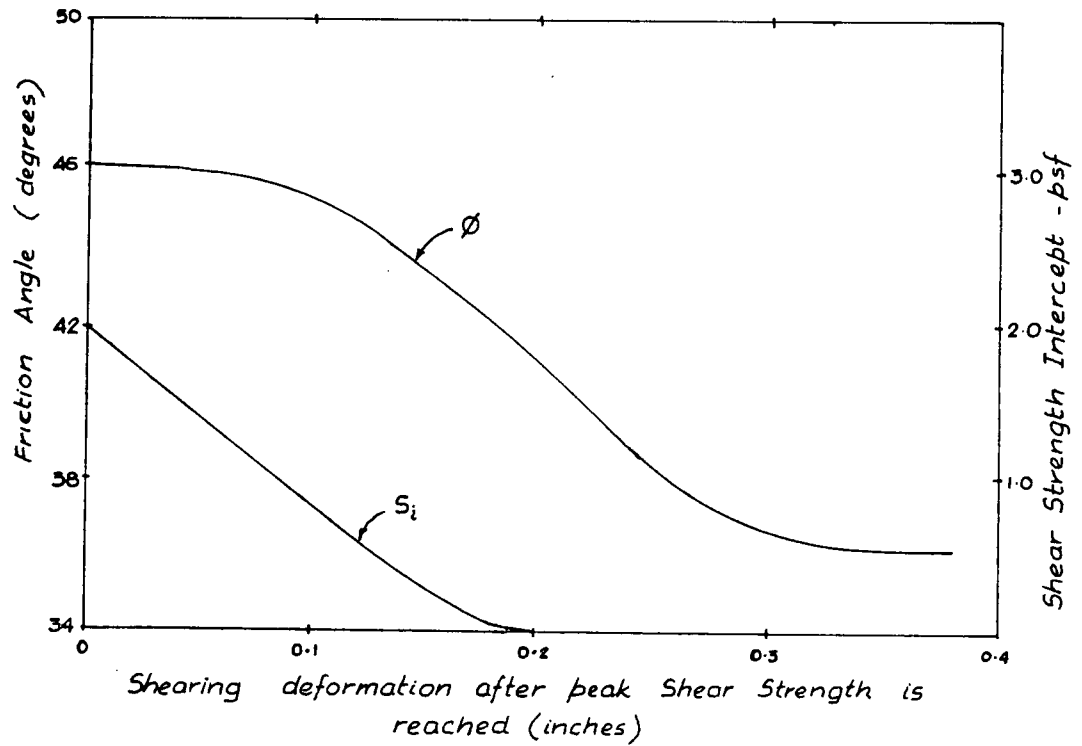
Fig.2.5 Loss of Shear Strength with Increasing
Deformation for Crushed Granite, No.4
through No.8 Size (Goodman and Seed,
1966)

include this variation. However, Goodman and Seed calculated their displacements by double integrating the acceleration in excess of the yield acceleration,

$$\ddot{u} = B(x) \ [\ k(t) - k_y(t) \ ] \tag{2.9}$$

where, $B(x) = g \ (\ Sin \ i \ tan \ \phi_{eq} + Cos \ i \ )$ (2.10)

and by using Figure 2.5 to get the variation of ϕ_{eq} with the displacement.

This method is presented on the assumption that the soil is sufficiently dry or sufficiently coarse grained in many cases, for capillary action and pore water pressure effects to be neglegible. Hence it is impossible to use the method to predict displacement in an environment where pore water pressure dominates, such as an offshore slope.

Seed (1966) pointed out that the calculation of the yield acceleration in a saturated cohesionless soil can only be made when the pore water pressures, under the deformation conditions induced by the earthquake can be reliably predicted.

An attempt to include the effect of pore water pressures in a rigid body type analysis was made by Sarma (1975). As this method is chosen as appropriate to modify for offshore use, it is completely discussed, with the modification, in Chapter 3. The author and Pender (1982), presented another rigid body analysis procedure, which will be

discussed in Chapter 4, to overcome some of the drawbacks in Sarma's method.

2.3.2. Deformable Body type analysis.

When an earthquake is originated at the bedrock level, amplification of the acceleration takes place through the soil strata, towards the surface. In a rigid body type analysis, this amplification is not taken into account. Furthermore, as the complete mass of soil is treated as a non deformable body, the relative motion which occurs over the entire depth is always neglected. Hence, a growing attention is now paid to deformable body type analyses.

Seed and Martin (1966) presented a method of calculating earthquake induced displacements of an earth slope of any soil type. Instead of calculating a single seismic coefficient in a pseudo-static analysis, a dynamic seismic coefficient is calculated by using a shear slice approach. The distribution of acceleration with the height is determined by assuming a constant shear modulus and a constant viscous damping coefficient and by summing up the response for the first six modes of vibration. Calculations were done following the analysis proposed by Mononobe et al.(1936), and the destribution of accelerations were determined for constant time intervals. An average seismic coefficient is then calculated by

$$k_{av} = F \: / \: W \qquad\qquad (2.11)$$

where, F is the total lateral force acting on the sliding

mass (Fig. 2.6), and

W is the weight of the sliding mass

Calculation is further simplified by representing the
potential sliding mass by a triangular wedge (Fig. 2.7). The
shear force at the base of the wedge is calculated and divided
by the weight of the wedge to get the average acceleration. For
a rigid body type analysis, these values are the "Dynamic
Average Accelerations". It has been found that the average
seismic coefficients vary considerably for different positions
of the soil wedges considered, with higher values being
developed with increasing height of the wedge within the
embankment. Time histories of these average coefficients were
plotted and then were approximated by an equivalant number of
seismic coefficient cycles of constant amplitude (Fig. 2.8).
These seismic coefficients can then be used to calculate the
displacements.

Ambraseys and Sarma (1967), used essentialy the same
method as Seed and Martin (1966). They presented their results
as a plot giving the variation of $k_{max}/\ddot{u}_{max}$ with depth of the
sliding wedge, where k_{max} is the maximum average acceleration at
the depth considered and $\ddot{u}_{max}$ is the maximum average crest
acceleration. It can easily be seen that both Seed and Martin
(1966) and Ambraseys and Sarma (1967), end up with similar
results (Fig. 2.9).

Makdisi and Seed (1978), again calculated an average
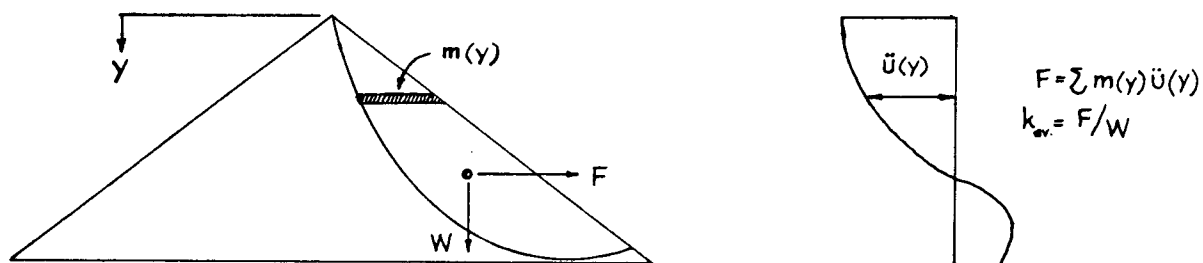
Fig.2.6   Average Seismic Coefficient (Seed and
          Martin, 1966)
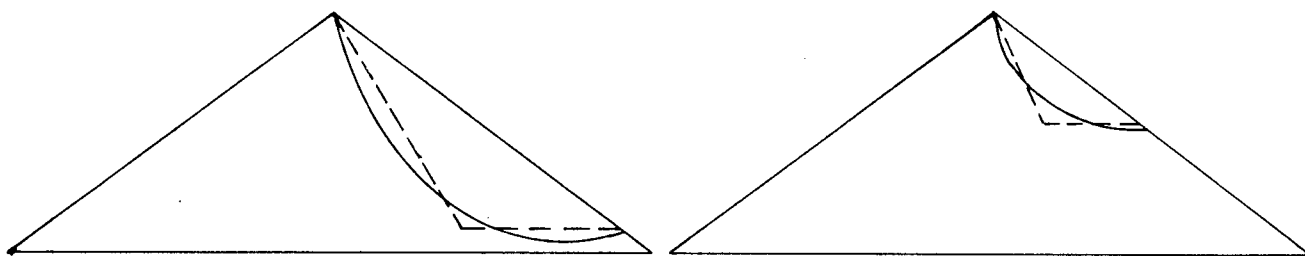
Fig.2.7   Approximation of Sliding Mass by a
          Triangular Wedge
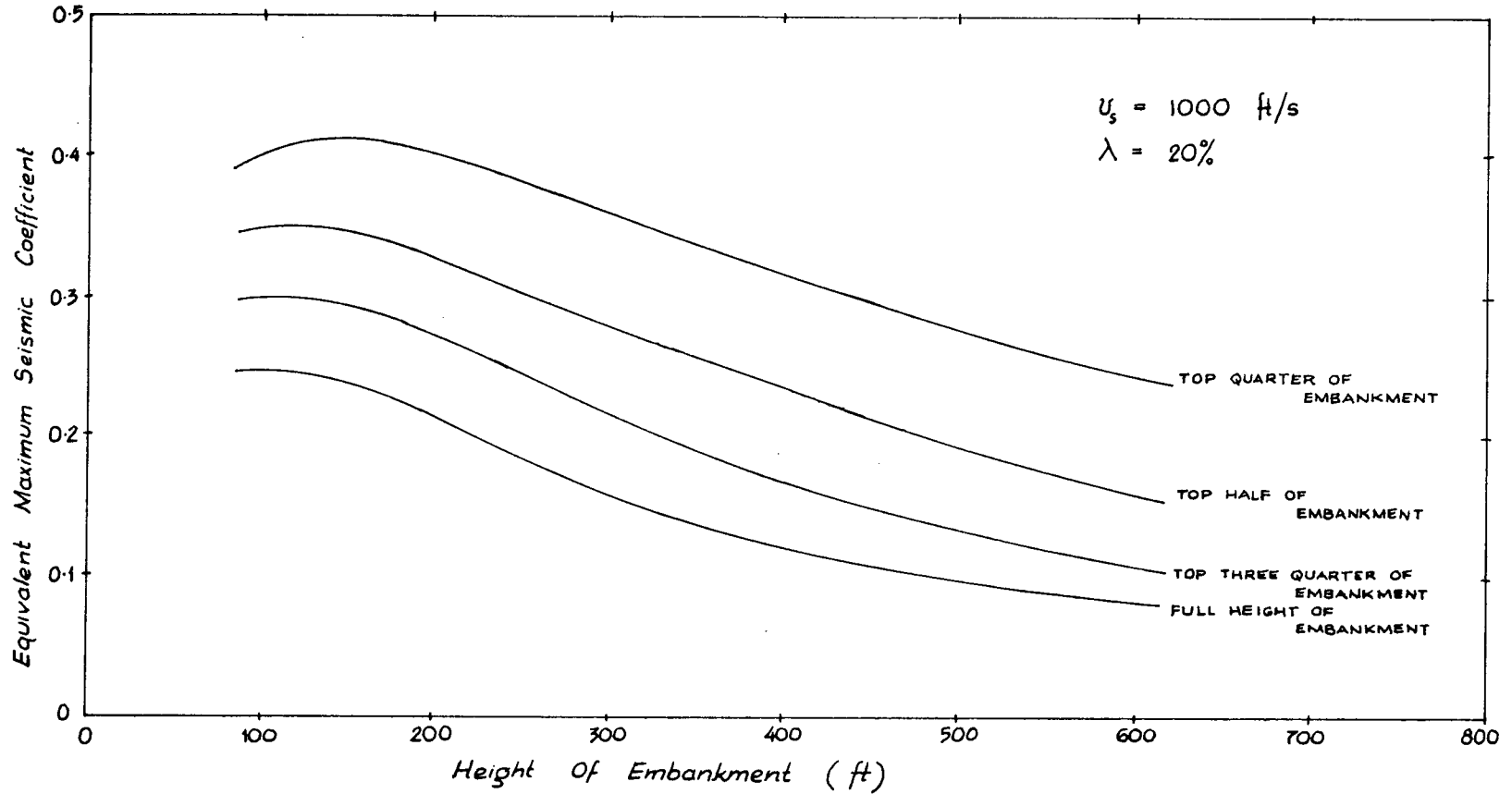
Fig.2.8   Values of Equivalant Maximum Seismic
          Coefficient for Homogeneous Embankments
          Subjected to El Centro Earthquake Motion
          (Seed and Martin, 1966)
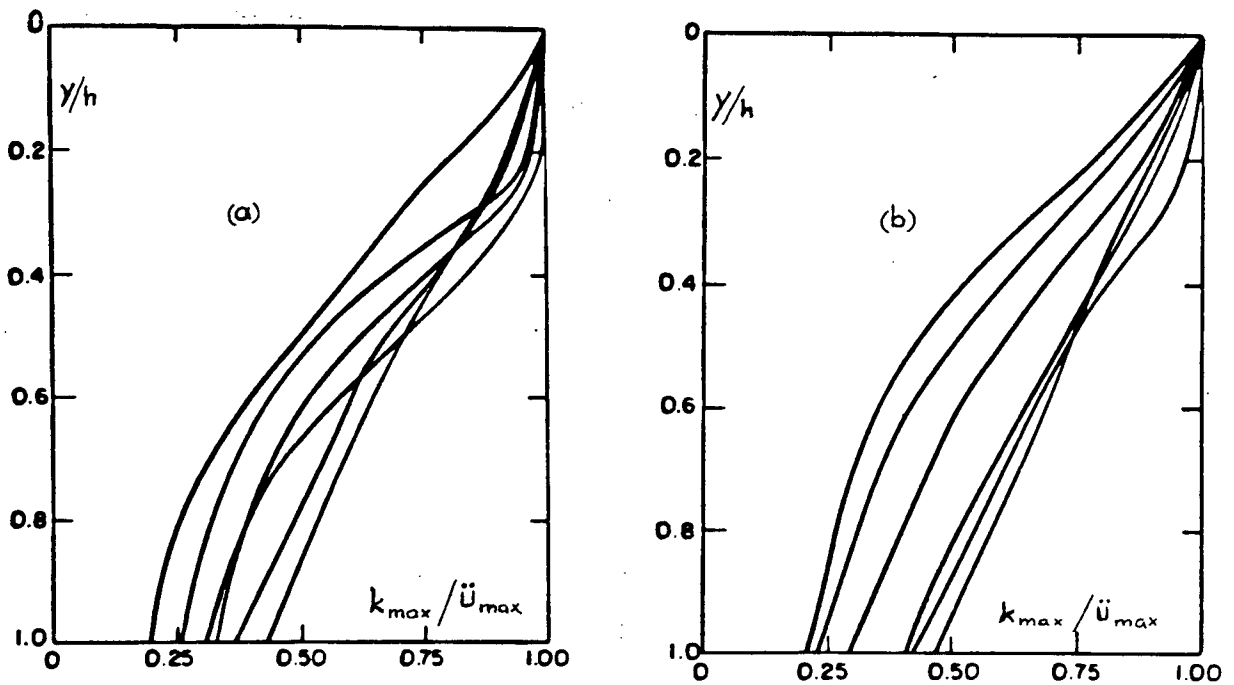
Fig.2.9   Variation of Ratio of Maximum Average
           Acceleration to Maximum Crest Acceleration
           with Depth of Sliding Surface
                 (a) El Centro Earthquake, data from
                     Martin (1965)
                 (b) Average of 8 Strong Motion
                     Earthquakes, data from Ambraseys
                     and Sarma (1967)

seismic coefficient at various depths of the embankment by the use of a finite element analysis. A critical failure surface is chosen and the stresses are calculated for a certian acceleration input at the base. By the use of the stresses on those finite elements which are along the failure surface, the total force acting on that particular failure mass is calculated (Fig. 2.10). Average acceleration is determined by taking the ratio of this force to the weight of the sliding mass. Makdisi and Seed (1978), used the finite element computer programme QUAD-4, with strain dependent modulus and damping. This programme uses Rayleigh damping and allows for variable damping to be used in different elements.

The results of Seed and Martin (1966), Ambraseys and Sarma (1967) and Makdisi and Seed (1978) are compared on the $y/h-k_{max}/\ddot{u}_{max}$ plane and a fairly good agreement is seen (Fig. 2.11).i.e.,both shear slice method and the finite element method yield almost the same acceleration pattern. Seed (1979), suggests to use the average curves given in Fig. 2.11, for design purposes. However, the design curves are not valid for low values of yield accelerations ($k_y/k_{max} < 0.01$) as the basic assumptions used in the finite element method , i.e.,the equivalent linear behaviour and small strain theory, are violated at these levels of accelerations.

Makdisi and Seed (1978) calculated the corresponding displacements by double integration, assuming a horizontal sliding surface. Similar computations were made by Ambraseys
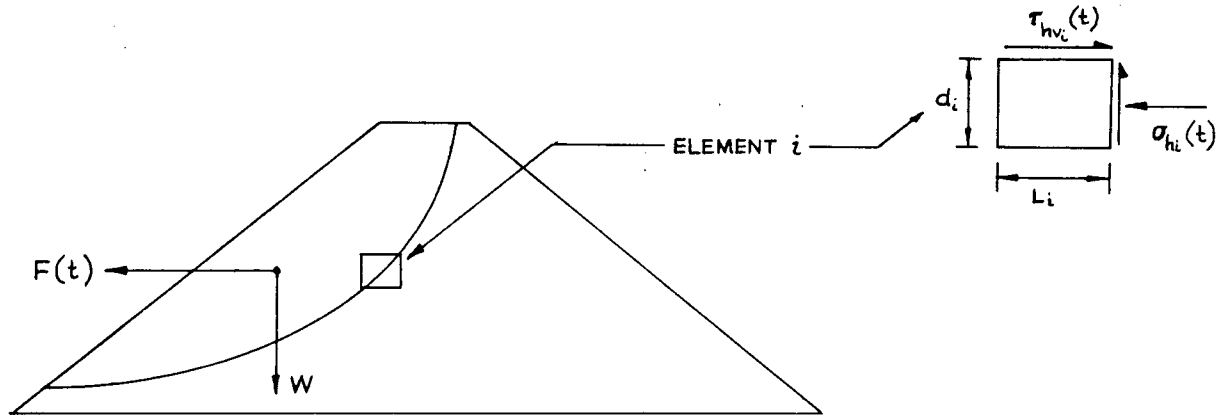
$$F(t) = \sum_{i=1}^{n} \tau_{hv_i}(t) \cdot L_i + \sigma_{hi}(t) \cdot d_i$$

n = NUMBER OF ELEMENTS ALONG THE SLIDING SURFACE

$$k_{av}(t) = F(t)/W$$

Fig.2.10 Calculation of Average Acceleration
from Finite Element Response Analysis
(Makdisi and Seed, 1978)

(1973) and Sarma (1975). Displacements are plotted against k_y/k_{max}, of an earth embankment subjected to magnitude 6-1/2 earthquake (Fig. 2.12). Makdisi and Seed (1978), adopted a normalization procedure to reduce the scatter and the normalised displacements are presented for earthquakes of magnitudes 6-1/2, 7-1/2 and 8-1/4 (Fig. 2.13).

Seed (1979) pointed out that the preceeding analysis methods proves that the pseudo-static analysis procedure proposed by Newmark can be used succesfully to calculate earthquake induced displacements in slopes. This method, however, is valid only if the soils do not lose more than 15% of their initial strength due to earthquake shaking. Vulnerability of the particular soil involved to loose its strength has to be assessed correctly before using these methods in designs. Seed (1979) suggests using a careful laboratory study to provide such information in cases of doubt.

Pseudo-static method of analysis, in whatever form used, cannot be applied for a slope made up of saturated cohesionless soils. A clearly defined yield strength cannot be found for loose to medium dense cohesionless soils. These soils will exhibit a progressive increase in pore water pressure as well as the strain, during cyclic loading. Continuous increase in pore water pressure may lead to cyclic mobility or even to liquefaction at a later stage, resulting in very large deformations. Moreover, once a loose or medium dense saturated sand slope is shaken by an earthquake, producing 100% pore
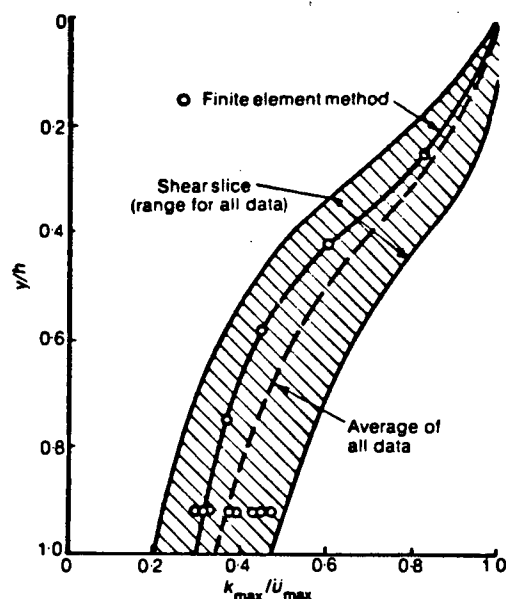
Fig.2.11 Variation of Effective Peak Acceleration
with the Depth of Potential Sliding Mass
(Makdisi and Seed, 1978)
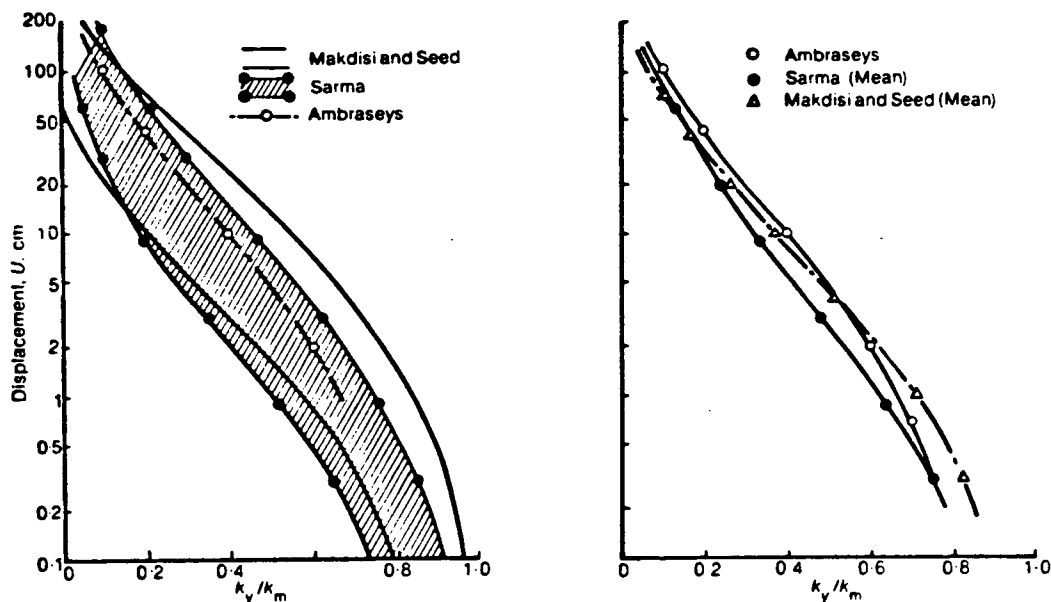
Fig.2.12 Computed Displacements for Embankment
Dams Subject to Magnitude 6 1/2
Earthquake for Soils which do not
Significantly Lose their Strength due to
Earthquake Shaking (Seed, 1979)
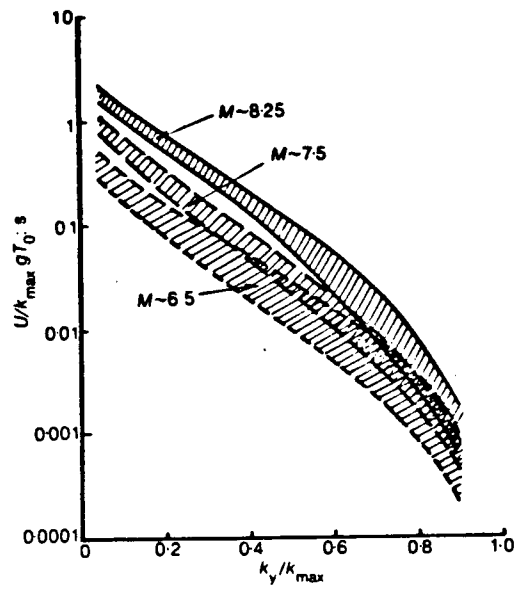
Fig.2.13 Computed Displacements of Embankment Dams
        for Soil Having Little or no Strength
        loss due to Earthquake Induced Deformation
        (Makdisi and Seed, 1978)

pressure ratio, deformations will be excessively increased under the next dynamic loading. This is demonstrated by Seed and Lee (1966) using cyclic triaxial test data.

An alternate procedure for the analysis of such slopes, which are vulnerable to a considerable loss in strength due to dynamic loading, was developed by Seed and his co-workers at the University of California, Berkely, and is summarized by Seed (1979) as follows.

(a) Determine the cross section of the soil structure to be used for analysis.

(b) Determine, with the cooperation of geologists and seismologists, the maximum time history of base excitation to which the structure and its foundation might be subjected.

(c) Determine as accurately as possible, the stress existing in the embankment before the earthquake; this is probably done most effectively at the present time using finite element analysis procedures.

(d) Determine the dynamic properties of the soils comprising the dam, such as shear modulus, damping characteristics, bulk modulus or Poisson's ratio, which determine its response to dynamic excitation. Since the material characteristics are non-linear, it is also necessary to determine how the properties vary with strain.

(e) Compute, using an appropriate dynamic finite element analysis procedure, the stresses induced in the embankment by the selected base excitation.

(f) Subject representative samples of the embankment materials to the combined effects of the initial static stresses and the superimposed dynamic stresses and determine their effects in terms of the generation of pore water pressures and the development of strains. Perform a sufficient number of these tests to permit similar evaluations to be made, by interpolation, for all elements comprising the embankment.

(g) From the knowledge of the pore pressures generated by the earthquake, the soil deformation characteristics and the strength characteristics, evaluate the factor of safety against the failure of the embankment either during or following the earthquake.

(h) If the embankment is found to be safe against failure, use the strains induced by the combined effects of static and dynamic loads to assess the overall deformations of the embankment.

(i) Be sure to incorporate the requisite amount of judgement in each of steps (a) to (b) as well as in the final assessment of probable performance, being guided by a thorough knowledge of typical soil characteristics, the essential details of finite

element analysis procedures, and a detailed
knowledge of the past performance of embankments in
other earthquakes.

In selecting the width of the cross section,
importance and the size of the problem has to be considered.
The number of sections to be analysed may be selected based on
the material zoning and geometry. The usual procedure is to use
the same finite element mesh for both static and dynamic
analyses. Mesh size is generally selected by experience and
judgement (Finn,1980). However, some of the dimensions might be
restricted by the computer programme used for the analysis.

Considerable care must be taken in selecting the
maximum time history of base accelerations to be used as the
input motion. This acceleration record should be consistent
with the geological conditions of the site and should be
selected according to the seismographic data produced by
seismologists. Frequency content, distance from the energy
source, and type of the foundation material are the main
factors to be considered.

A number of finite element procedures are available
to calculate state of stress existing in the embankment before
the earthquake. True non linear finite element methods,
incorporating hyperbolic or Ramberg-Osgood stress-strain
relations should be used for best results. In using these
programmes it is important to obtain the necessary soil

parameters by proper laboratory testing, simulating field conditions.

Dynamic analysis of the slope is carried out by using newly developed dynamic computer programmes. Most of these programmes are based on two major assumptions.

(1) Seismic excitation is primarily due to shear waves propagating vertically, and

(2) The non linear behaviour of soil may be approximated by a viscously damped linear elastic model in which the damping and stiffness are represented by strain dependent modulii and damping factors.

'SHAKE' is the first computer programme incorporating the equivalent linear method. It is also capable of introducing an energy transmitting boundary. Furthermore, it has provisions for applying input motion at any level. The analysis was further extended to two and three dimensions in the programmes QUAD-4, LUSH and FLUSH. 'QUAD-5S', a modified version of QUAD-4 is also available and is again based on equivalent linear method.

Finn et al.(1978) have indicated that the total stress analysis (all equivalent linear methods are total stress methods) overestimates the dynamic response of saturated sandy soils, when the pore water pressure ratio exceeds 30%. In addition, equivalent linear programmes do not take the effect

of increasing pore water pressure on soil stiffness into account. Furthermore, direct computation of the permanent deformations cannot be carried out with these programmes. Methods of converting strain potentials to strains or deformations are not verified for compatibility requirements.

Hence, dynamic analysis may be carried out by using true non linear computer programmes such as DESRA-1, DESRA-2 and CHARSOIL. DESRA-1 and DESRA-2 are one dimensional programmes, the latter including energy transmitting boundaries. These non linear programmes should be used wherever possible for better accuracy.

2.4 Available stability analysis methods for offshore slopes.

Two non-linear computer programmes are available for calculating the dynamic displacements of an offshore slope. The first programme, DONAL-2, was developed in 1981 by the soil dynamics group of the University of British Columbia. Second programme, DCHARMS, was developed by Moriwaki et al. in 1982.

2.4.1 DONAL-2

DONAL-2 (Dynamic One dimentional Non-linear Analysis of sloping soil Layers; Iai, Susumu and Finn, W. D. L., February 1982) was developed upon a request by ERTEC Western Incorporated, Long Beach, California, to analyse the stability of offshore slopes in Mediterranean sea, off the Spanish coast.

This programme analyses sloping soil layers, sand and/or clay, shaken by shear waves propagating at right angles to the slope ground surface, when the slope is formed of soil layers parallel to this surface. DONAL-2 is the first non-linear effective stress computer programme developed for the analysis of such slopes. Non-linearity and the hysteresis behaviour of the soil is taken into account by using a hyperbolic Masing stress-strain curve. The actual hysteresis loops are followed in analyses instead of using average properties such as the strain dependent secant modulii and equivalent viscous damping ratios. True non-linearity is ensured by taking the effects of increasing pore water pressure on soil stiffness into account. The pore water pressure model developed by Martin et al.(1975) was included in the effective stress analysis. Parameters in this model are evaluated by determining the pore pressure etc. in cyclic simple shear tests. Pore water pressures are adjusted, to take the effect of slope into account, by considering the static shear stress. Effect of finite rigidity at the base of the deposit is approximated by using a dashpot model to simulate the energy transmitting boundary. Furthermore, DONAL-2 takes the degradation of clay into account by using a degradation model similar to the one proposed by Idriss et al.(1976). The programme is capable of solving three main types of problems.

(a) OPTION 1 - dynamic response of a sloping soil

deposit is calculated, but the effect of pore water pressure is not included in the analysis.

(b) OPTION 2 - dynamic response of the deposit is calculated including the effect of pore water pressure generated due to cyclic loading. However, the pore water pressure calculated for each layer is assumed to be confined within the layer.

(b) OPTION 3 - this option includes calculations as for OPTION 2 and in addition, it includes the effects of redistribution and dissipation of pore water pressure, by the application of the consolidation-dissipation equation.

If all the layers are clay, the following option is also available.

(d) OPTION 4 - dynamic response analysis including the effect of degradation of clay.

2.4.2 DCHARMS

The true non-linear computer programme CHARSOIL was first modified by Idriss et al., by including degradation of clay. Moriwaki et al.(1982) modified this further, to analyse mildly sloping clay layers shaken by shear waves propagating perpendicular to the slope surface and the new programme was

designated DCHARMS.

In 1976, Idriss et al. introduced a new stress-strain
model for soft clays under cyclic loading, including stiffness
degradation. In this model, the hysterisis loop generated by a
cycle of loading flatterns out with increasing number of
cycles. The amount of degradation in each half cycle is assumed
to be a simple function of the total degradation until the
previous half cycle, and a t-parameter, which is determined by
the applied cyclic strain level. The computer programme DCHARM
was then developed by incorporating this stress-strain model in
the true non-linear computer programme CHARSOIL, which was
developed originally to analyse horizontal soil layers shaken
by vertically propagating shear waves. DCHARM takes degradation
into account by modifying the Ramberg-Osgood equation, used in
CHARSOIL, to define the backbone curve.

Moriwaki et al.(1982) considered the effect of
earthquakes on mildly sloping clay layers. A unique
relationship was assumed between the residual shear strain in
the downslope direction and the degradation index δ for the
purpose of calculating the displacements. As δ is repeatedly
calculated in the programme DCHARM, residual shear strain can
be determined at any instant and a simple integration produces
the downslope displacement.

It is important to note at this point that DCHARMS
can only handle clay slopes. DONAL-2, on the other hand, is
capable of handling either sand or clay.

CHAPTER 3

MODIFICATION OF SARMA'S METHOD.

Sarma (1975) developed a rigid body method of analysing slope stability under earthquakes. This method is capable of handling saturated or partially saturated soils which do not have any shear strength intercept at zero normal stress. This method can be modified for offshore slopes. A summary of the original method presented by Sarma is given, followed by the modification.

Sarma (1975), proposes to use the Newmark model to analyse the effect of the inertia force and the pore pressures on the factor of safety, critical acceleration, and the subsequent displacement during an earthquake. A cohesionless material which obeys Mohr-Coulomb failure criterion with effective stresses is chosen for the analysis. Pore pressure changes were introduced by the use of Skempton's pore pressure parameters, in the effective stress analysis.

The stability of a rigid block on a plane inclined surface is considered (Fig. 3.1). If the block and the plane are separated by a thin layer of cohesionless soil of internal

friction angle ϕ' and if the surface slope is i,
The total normal stress on the plane is

$$\sigma_0 = W \cos i \, / \, a \qquad (3.1)$$

and the shear stress is

$$\tau_0 = W \sin i \, / \, a \qquad (3.2)$$

where W and a are the weight and the base area of the
block respectively. As the material obeys Mohr-Coulomb
criteria, the factor of safety before the earthquake is given
by,

$$F_0 = \frac{\sigma'_0 \tan \phi'}{\tau_0} = \left(\cos i - \frac{u_0 a}{W} \right) \frac{\tan \phi'}{\sin i} \qquad (3.3)$$

where σ'_0 and u_0 are the initial effective stress and
the initial excess pore pressure respectively.

Let an earthquake acceleration kg act on the base at
an angle θ to the horizontal. Assuming rigid body motion (i.e.
seismic coefficient = 1), this will produce a force of kW on
the block with the same inclination as the acceleration (Fig
3.2). The total normal stress during the pulse is

$$\sigma = W \, [\, \cos i - k \sin (i - \theta)] \, / \, a \qquad (3.4)$$

$$\sigma_o = W \, Cos \, i \, / \, a$$

$$\tau_o = W \, Sin \, i \, / \, a$$
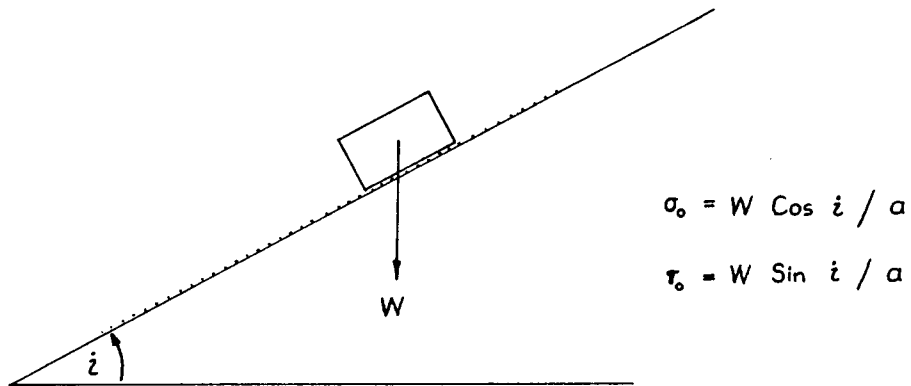
Fig.3.1   The Model Considered by Sarma (1975)
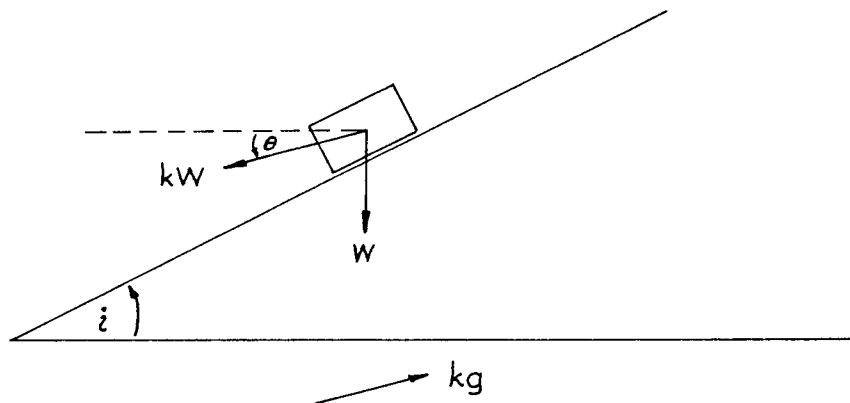
Fig.3.2   The Model in Figure 3.1, with Earthquake
          Indced Acceleration

and shear stress is

$$\tau = W [\text{Sin } i + k \text{ Cos } (i - \theta)] / a \qquad (3.5)$$

reducing the factor of safety to

$$F = [\text{Cos } i - k \text{ Sin}(i-\theta) - (u_0 a/W)]\tan \phi / (\text{Sin } i + k \text{ Cos}(i-\theta)) \qquad (3.6)$$

where $u = u_0 + \Delta u$ \qquad (3.7)

and Δu = increase in excess pore water pressure due to the inertia force produced by the acceleration pulse.

When the factor of safety becomes unity, failure occurs and the corresponding kg will be the yield acceleration for the block.

F=1 yields,

$$k = \frac{[\text{Cos } i - (u_0 a/W) - (\Delta u a/W)]\tan \phi - \text{Sin } i}{\text{Cos } (i - \theta) + \text{Sin } (i - \theta) \tan \phi} \qquad (3.8)$$

However, before k can be calculated, the term $\Delta u a/W$ must be determined. Pore pressure increase is calculated by Skempton's pore pressure equation and hence it is necessary to evaluate changes in principal stresses during the earthquake acceleration. As the stress state at a point is completely defined by Mohr's circle of stresses, Sarma introduced a hypothesis at this stage, to draw the Mohr's circle. The

necessity of such a hypothesis is obvious as the stresses on only one plane are known and as one point is not sufficient to define the circle. According to Sarma's hypothesis, if σ' and τ are the effective normal and shear stresses on a possible failure plane and F is the factor of safety, the state of stress at any point along the failure surface would be the same as if the friction angle of the material were $\psi = \tan^{-1} (\tan \phi/F)$ It should be noted that this results in a ψ angle equal to the slope angle, under the initial stress conditions, if there is no initial excess pore water pressure.

The Mohr's circle is drawn with the aid of this hypothesis and is given in Figure 3.3. Solid lines are effective stress circles and dotted lines are total stress circles. Effective principal stresses on the surface before the earthquake acceleration are,

$$\sigma'_{10} = \sigma'_0 + \tau_0 (\tan \psi_0 + \text{Sec } \psi_0)$$

$$\sigma'_{30} = \sigma'_0 + \tau_0 (\tan \psi_0 - \text{Sec } \psi_0)$$

$$(3.9)$$

where $\quad \psi_0 = \tan (\tan \phi'/F_0)$ $\hspace{3cm}$ (3.10)

similarly, at failure, i.e. F=1 and $\psi = \phi'$

$$\sigma'_1 = \sigma' + \tau (\tan \phi' + \text{Sec } \phi')$$

$$\sigma'_3 = \sigma' + \tau (\tan \phi' - \text{Sec } \phi')$$

$$(3.11)$$

Total stress changes,

$$\Delta\sigma_1 = (\sigma'_1 + u) - (\sigma'_0 + u_0)$$

$$= \sigma - \sigma_0 + \tau(\tan\phi' + \sec\phi') - \tau_0(\tan\psi_0 + \sec\psi_0)$$

or $\quad \Delta\sigma_1 a/W = -k \sin(i-\theta) + [\sin i + k \cos(i-\theta)][\tan\phi + \sec\phi]$

$$-\sin i(\tan\psi_0 + \sec\psi_0) \quad (3.12)$$

similarly,

$$\Delta\sigma_3 a/W = -k \sin(i-\theta) + [\sin i + k \cos(i-\theta)][\tan\phi - \sec\phi]$$

$$-\sin i(\tan\psi_0 - \sec\psi_0) \quad (3.13)$$

using Skempton's pore pressure equation,

$$\Delta u = B [\Delta\sigma_3 + A (\Delta\sigma_1 - \Delta\sigma_3)] \quad (3.14)$$

or $\quad \Delta u a/W = B(-k \sin(i-\theta) + [\sin i + k \cos(i-\theta)][\tan\phi$

$$+ (2A-1)\sec\phi] - \sin i[\tan\psi_0 + (2A-1)\sec\psi_0])$$

$$(3.15)$$

by substituting in equation 3.8 and rearranging terms,

$$k = \frac{\cos i}{\cos(i-\theta)} \times \frac{\tan\phi - \tan i - (u_0 a\tan\phi/\cos i) - B\tan i\tan\phi[C - \tan\psi_0]}{1 + \tan(i-\theta)\tan\phi + B\tan\phi[\tan\phi - \tan(i-\theta) - (1-2A)\sec\phi]} \quad (3.16)$$

where $\quad C = \tan\phi - (1-2A)(\sec\phi - \sec\psi_0) \quad (3.17)$

If the acceleration is horizontal, $\theta = 0°$

$$k = \frac{\tan\phi - \tan i - (u_0 a \tan\phi / \cos i) - B\tan i \tan\phi [C - \tan\psi_0]}{1 + \tan i \tan\phi + B\tan\phi [\tan\phi - \tan i - (1 - 2A)\sec\phi]} \quad (3.18)$$

If $u_0 = 0$, i.e., if there is no initial excess pore water pressure,

$$k = \frac{\tan\phi - \tan i - B\tan i \tan\phi [\tan\phi - \tan\psi_0 - (1 - 2A)(\sec\phi - \sec\psi_0)]}{1 + \tan i \tan\phi + B\tan\phi [\tan\phi - \tan i - (1 - 2A)\sec\phi]} \quad (3.19)$$

for dry soil, $B = 0$ and hence,

$$k = \tan(\phi - i) \quad (3.20)$$

which is Seed and Goodman's expression for dry cohesionless soils.

Modification of the preceeding analysis for underwater slopes is not too difficult. Following the same procedure, but including water force due to submergence (Fig. 3.4), and assuming that there is no initial excess pore water pressure for simplicity, initial stresses on a plane parallel to the slope surface will be given by,

$$\sigma_0 = (1 - \rho_\omega/\rho) \, W \cos i \, / \, a$$
$$\tau_0 = (1 - \rho_\omega/\rho) \, W \sin i \, / \, a \quad (3.21)$$

i.e. there is no change in the initial factor of safety, F. However, these stresses will change to,
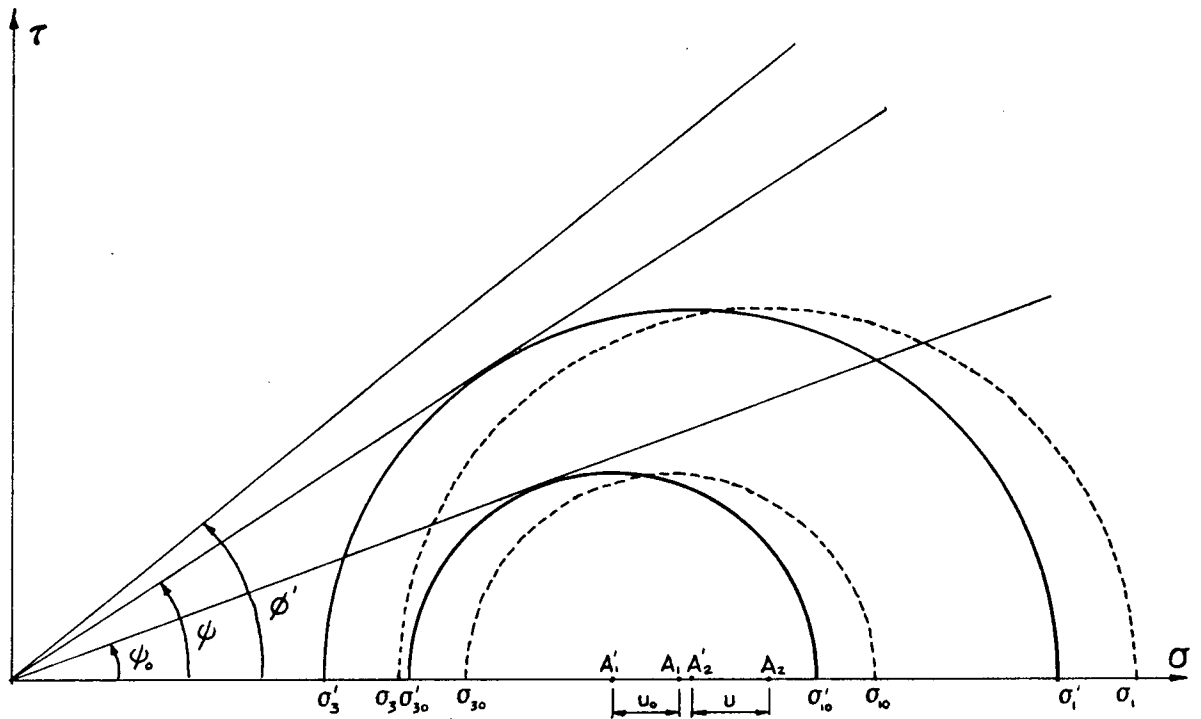
Fig.3.3   Mohr's Circles using Sarma's Hypothesis
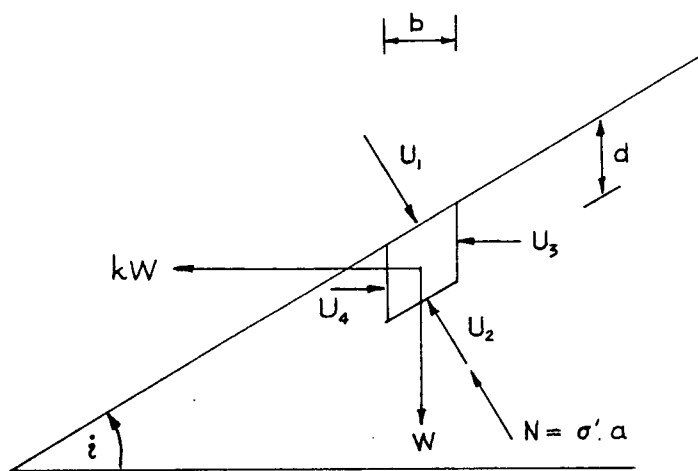
Fig.3.4   Forces on a Submerged Block

$$\sigma = [(1 - \rho_\omega/\rho) \text{ Cos i } - \text{ k Sin i}] \text{ W } / \text{ a} \qquad (3.22)$$

$$\tau = [(1 - \rho_\omega/\rho) \text{ Sin i } + \text{ k Cos i}] \text{ W } / \text{ a}$$

during the horizontal acceleration kg.

If, $k' = k /(1 - \rho_\omega/\rho)$ \qquad (3.23)

equations 3.22 will reduce to,

$$\sigma = (1 - \rho_\omega/\rho)(\text{Cos i } - \text{ k' Sin i}) \text{ W } / \text{ a}$$
$$\tau = (1 - \rho_\omega/\rho)(\text{Sin i } + \text{ k' Cos i}) \text{ W } / \text{ a} \qquad (3.24)$$

Hence, the change in stresses due to earthquake inertia forces can be represented by a line perpendicular to the in-situ effective stress line (Fig. 3.5), in a $\tau - \sigma$ diagram. Comparing the equations 3.4 and 3.5 with equation 3.24, and considering only the horizontal accelerations, it is clear that the critical acceleration k will be given by

$$k' = \frac{\tan\phi - \tan i - B\tan i\tan\phi[\tan\phi - \tan\psi_0 - (1-2A)(\text{Sec}\phi - \text{Sec}\psi_0)]}{1 + \tan i\tan\phi + B\tan\phi[\tan\phi - \tan i - (1-2A)\text{Sec}\phi]} \qquad (3.25)$$

where $k' = k /(1 - \rho_\omega/\rho)$

as the typical values of $(1 - \rho_\omega/\rho)$ range between 0.4 and 0.6, it is readily apparent that the critical acceleration for an underwater slope is roughly one-half of that for a non

$$k' = k \left/ \left(1 - \rho_w/\rho \right) \right.$$
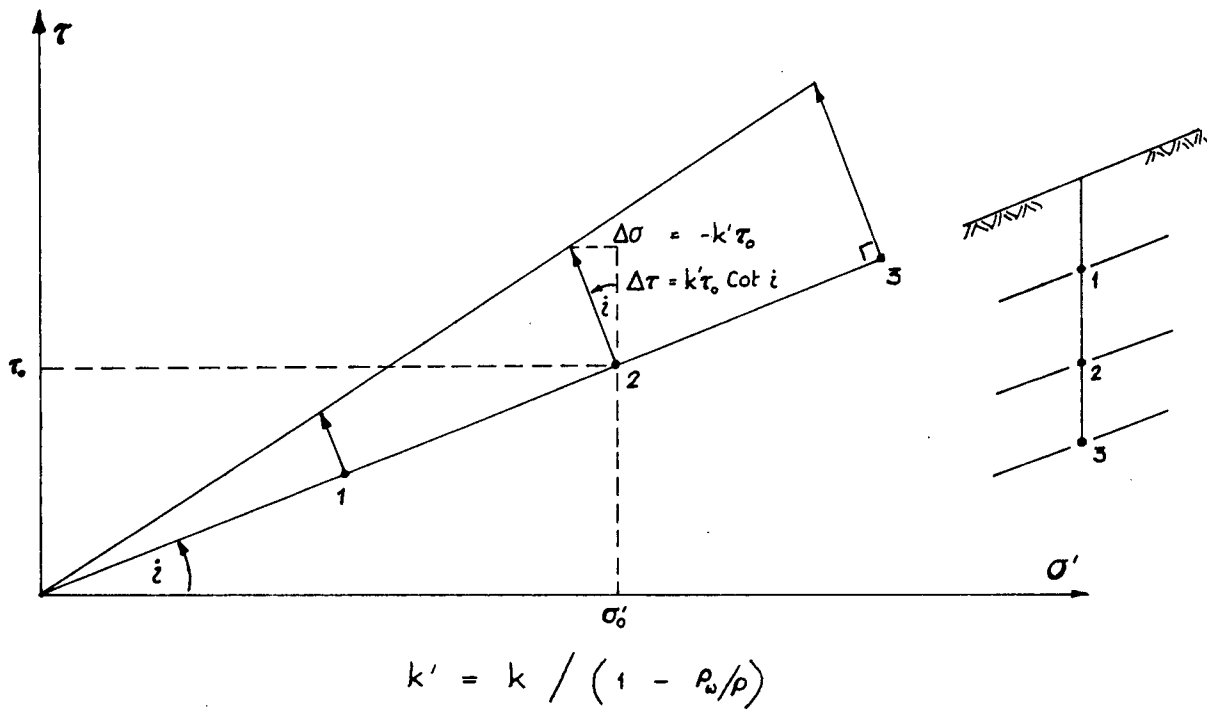
Fig.3.5   Stress Increments due to the Earthquake
Inertia Force

submerged slope with the same soil properties.

for B = 0, k = $(1 - \rho_\omega/\rho) \tan(\phi - i)$ (3.26)

    $i = \phi°$, k = 0   ·   (3.27)

    $i = 0°$, k = $(1 - \rho_\omega/\rho) \tan\phi/(1 + B \tan\phi(\tan\phi+(2A-1) \operatorname{Sec}\phi))$

                                                         (3.28)

       The limitations, advantages and disadvantages of the method will be discussed in the next chapter, along with Pender's model.

CHAPTER 4

PENDER'S MODEL.

As discussed in Chapter 3, Sarma (1975) introduced a
new hypothesis to draw the Mohr's circle of stresses. According
to this hypothesis the state of stress at any point along the
failure surface will be the same as if the friction angle of
the material were $\psi = \tan^{-1} (\ \tan \phi' \ / \ F)$, where F is the
corresponding factor of safety. The Mohr circle is then drawn
with the help of this hypothesis. However, Sarma did not pay
any attention to the subsequent rotation of principal stress
directions.

Principal stresses will be vertical and horizontal
for a level ground surface as there is no shear stress on the
horizontal surface. Major principal stress will be somewhat off
vertical for a sloping soil surface. Following Sarma's
hypothesis, this inclination can be calculated. As pointed out
earlier, for the in-situ stress state, Sarma's hypothesis is
the same as assuming that the Mohr circle for this stress state
is tangent to a line making an angle equal to the slope angle,
in the $\tau - \sigma$ plane, if there is no initial excess pore water
pressure. Hence, for a slope angle $i°$, major principal stress
will be $(45 - i/2)°$ off vertical (Fig. 4.1). This, not only

indicates that the inclination of the major principal stress to the vertical decreases with increasing slope, but also leads to a rather high rotation even for very small slope angles. For example: for a slope of $10°$, major principal stress is $40°$ off vertical, which is remarkably high for such a small slope angle.

In addition to the principal stress rotation, it is worth examining the ratio of principal stresses. For a horizontal soil surface, ratio of minor principal stress to the major principal stress is denoted by K_0, the coefficient of earth pressure at rest. For a normally consolidated clay, K_0 is approximately equal to $1 - \mathrm{Sin}\phi'$, where ϕ' is the internal friction angle of the clay. Following Sarma's hypothesis, if we denote principal stress ratio by K_0, it can be shown that (Fig. 4.2), under the in-situ stress conditions,

$$K_0 = (1 - \mathrm{Sin}\ i)/(1 + \mathrm{Sin}\ i) \qquad (4.1)$$

This expression, being independent of friction angle, will give the same value of K_0 for any type of soil, but with the same slope geometry.

Having recognized these drawbacks in Sarma's hypothesis, Pender introduced a new hypothesis to draw the Mohr's circle of stresses for in-situ stress state, based on an assumed equation for the ratio of principal stresses. Assuming,
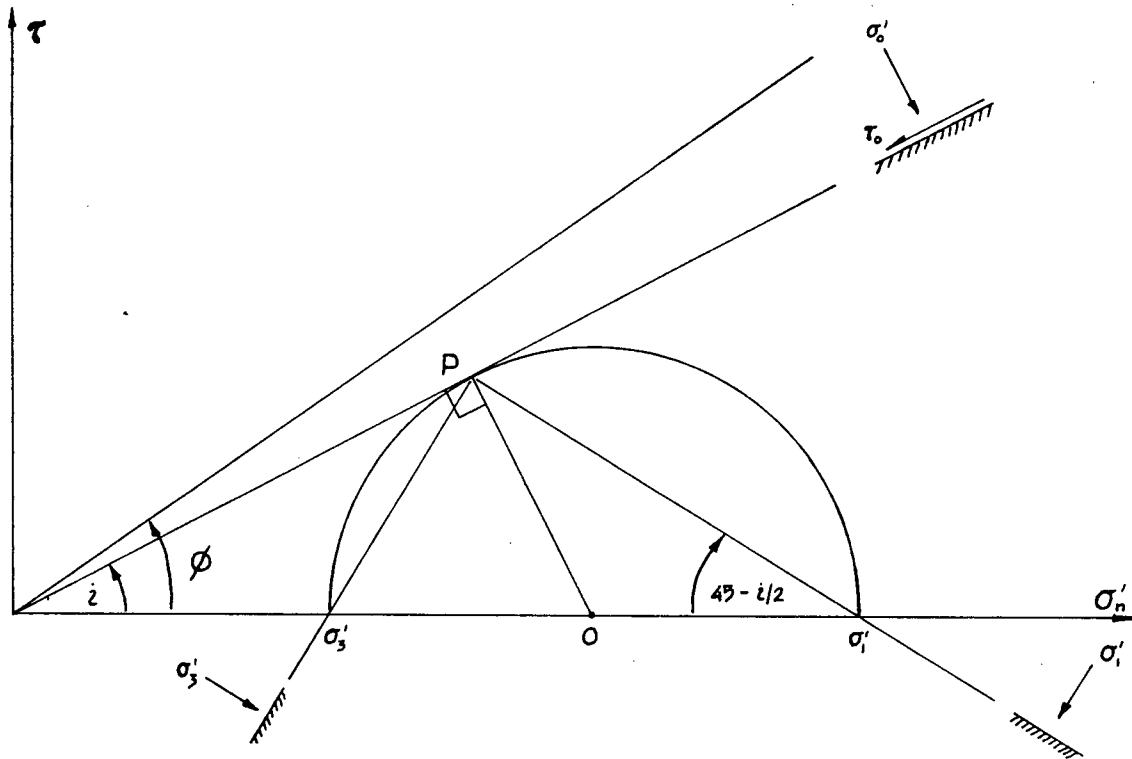
Fig.4.1   Inclination of Principal Stresses -
Sarma's Hypothesis

$$\frac{\sigma_1'}{\sigma_3'} = \frac{1 + \text{Sin } i}{1 - \text{Sin } i}$$
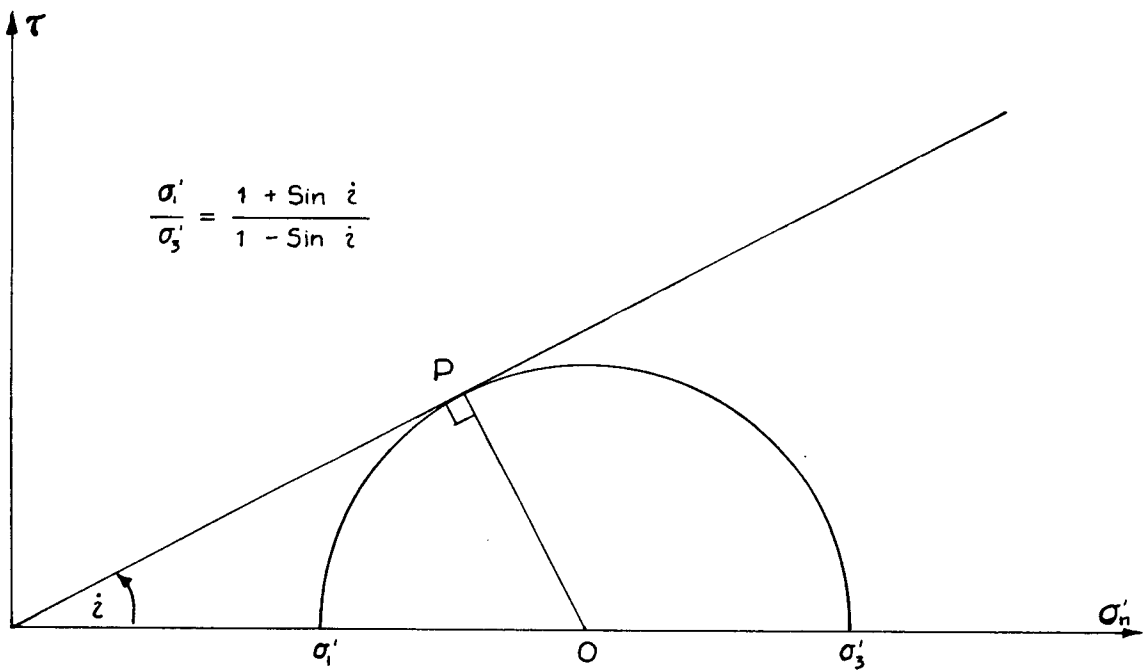
Fig.4.2   Principal Stress Ratio - Sarma's Hypothesis

$$K_0 = (1 - \sin \phi')/(1 + \sin i) = \sigma'_{30}/\sigma'_{10} \qquad (4.2)$$

he constructed his Mohr circle for in-situ stress state, which gave a higher mobilized friction angle than the slope angle for the case of zero initial excess pore water pressure (Fig. 4.3). The use of equation 4.2 as the principal stress ratio is justified at two inclinations of the slope. For $i = 0^\circ$, equation 4.2 will reduce to the familiar approximate equation for horizontal ground, $K_0 = 1 - \sin \phi'$ and for $i = \phi'$, i.e., at failure, K_0 will be the principal stress ratio for the failure Mohr circle.

The stresses on a plane parallel to the slope surface will be given by (Fig. 4.3, Mohr circle for the in-situ stress conditions),

$$\sigma'_{n0} = 1/2(\sigma'_{10}+\sigma'_{30}) + 1/2(\sigma'_{10}-\sigma'_{30}) \cos 2\beta$$
$$\tau_0 = \qquad\qquad 1/2(\sigma'_{10}-\sigma'_{30}) \sin 2\beta \qquad (4.3)$$

Substituting for σ'_{30} by 4.2,

$$2\sigma'_{n0} - (1 + K_0)\sigma'_{10} = (1 - K_0)\sigma'_{10} \cos 2\beta$$
$$2\tau_0 = (1 - K_0)\sigma'_{10} \sin 2\beta \qquad (4.4)$$

squaring and adding,

$$4\sigma'^2_{n0}-4(1 + K_0)\sigma'_{n0}\sigma'_{10}+ (1 + K_0)^2\sigma'^2_{10} + 4\tau_0^2= (1 - K_0)^2\sigma'^2_{10}$$

but, as $\tau_0=\sigma'_{10}\tan i$ (equation 3.20), this will reduce to,

$$4\sigma_{no}'^2 - 4(1 + K_0)\sigma_{10}'\sigma_{no}' + (1 + K_0)^2\sigma_{10}'^2 + 4\sigma_{no}'^2\tan^2 i = (1 - K_0)^2\sigma_{10}'^2$$

$$K_0\sigma_{10}'^2 - 4(1 + K_0)\sigma_{10}'\sigma_{nd}' + \sigma_{no}'^2\sec^2 i = 0$$

or $\quad \sigma_{10}' = \sigma_{no}'[(1 + K_0) \pm \sqrt{(1 + K_0)^2 - 4K_0\sec^2 i}]/2K_0$

$\quad \sigma_{10}'/\sigma_{no}' = [(1 + K_0) \pm \sqrt{(1 + K_0)^2 - 4K_0\sec^2 i}]/2K_0$

smaller root gives the lesser principal stress rotation. Hence,

$$\sigma_{10}'/\sigma_{no}' = [(1 + K_0) - \sqrt{(1 + K_0)^2 - 4K_0\sec^2 i}]/2K_0 \qquad (4.5)$$

and

$$\sin 2\beta = \frac{2\tau_0}{(1 - K_0)\sigma_{10}'} = \frac{4K_0\tan i}{(1-K_0)[(1+K_0)-\sqrt{(1+K_0)^2-4K_0\sec^2 i}]} \qquad (4.6)$$

By examining Figure 4.3 , it is clear that the major principal stress will be $(\beta - i)^\circ$ off vertical.
mobilized friction angle ψ will be given by,

$$\sin\psi = (\sigma_1' - \sigma_3')/(\sigma_1' + \sigma_3') = (1 - K_0)/(1 + K_0) \qquad (4.7)$$

The new value of mobilized friction angle ψ° and the inclination of major principal stress to the vertical $(\beta - i)^\circ$, is tabulated in Table 1. for a cohesionless soil having an internal friction angle of 25° and for a slope angle varying from 0° to 25° . Inclination of major principal stress to the vertical is more acceptable than the values given by Sarma's hypothesis. Taking the same example considered before

($i = 10^o$, $\phi' = 25^o$), principal stress is only 10.3^o off vertical, compared to 40° obtained by using Sarma's method.

Skempton's pore pressure equation was again used to calculate the pore pressure increment due to the inertia force produced by an earthquake acceleration pulse. An earthquake acceleration k which brings the effective stress mohr circle to the failure state (assuming a Mohr-Coulomb failure criteria) will be the critical acceleration (Fig. 4.4). This can be calculated as below.

It was shown that the ratio of major principal stress to the normal stress on a plane parallel to the slope surface is given by,

$$\sigma'_{10}/\sigma'_{n0} = [(1 + K_0) - \sqrt{(1 + K_0)^2 - 4K_0 \sec^2 i}]/2K_0 \qquad (4.5)$$
$$= Q \text{ , say.} \qquad (4.8)$$

under in-situ stress conditions. If there is no initial pore water pressure, principal stresses will be given by,

$$\sigma'_{10} = Q\tau_0 \cot i$$
$$\sigma'_{30} = QK_0\tau_0 \cot i \qquad (4.9)$$

where, τ_0 is the initial shear stress on a plane parallel to the slope surface
principal stresses after the application of earthquake inertia force kg, are
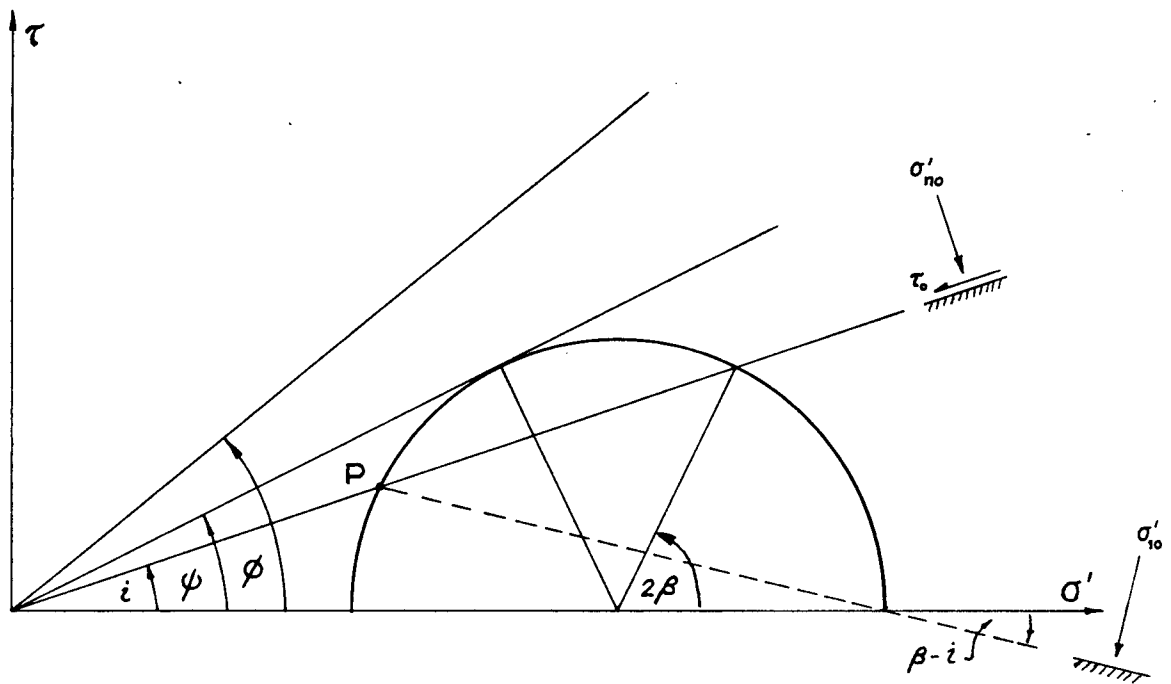
Fig.4.3 Mohr Circle for In-situ Stress Conditions
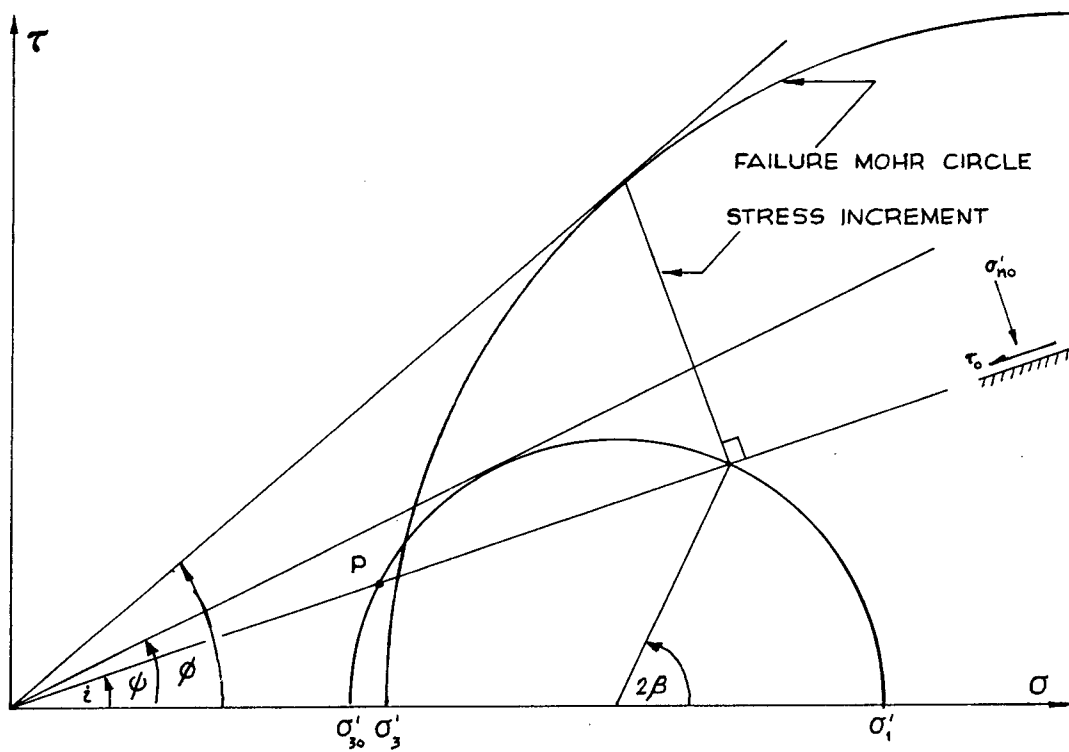
Fig.4.4 Failure Mohr Circle

TABLE 1

MOBILIZED FRICTION ANGLE AND THE PRINCIPAL STRESS ROTATION FOR
VARYING SLOPE ANGLES

ψ is the mobilized friction angle

$(\beta - i)°$ is the principal stress rotation

internal friction angle of the soil = 25°

i	K	$\psi°$	$\beta°$	$(\beta-i)°$
0	0.5774	15.5	0.0	0.0
5	0.5311	17.8	10.8	5.8
10	0.4920	19.9	20.3	10.3
15	0.4587	21.8	29.6	14.6
20	0.4302	23.5	39.6	19.6
22.5	0.4176	24.3	44.4	21.9
24.0	0.4105	24.71	50.4	26.4
24.5	0.4081	24.86	52.5	28.0
25.0	0.4059	25.00	57.5	32.5

$$\sigma_1 = (\sigma'_{no}-k'\tau_0)+\tau_0(1 + k' \operatorname{Cot} i)(\tan \phi'+ \operatorname{Sec} \phi')$$

$$\sigma_3 = (\sigma'_{no}-k'\tau_0)+\tau_0(1 + k' \operatorname{Cot} i)(\tan \phi'- \operatorname{Sec} \phi') \quad (4.10)$$

at failure

where, $k'= k/(1 - \rho_\omega/\rho)$

giving,

$$\Delta\sigma_3 = \tau_0[\tan \phi'- \operatorname{Sec} \phi'+ \operatorname{Cot} i(1 - K_0 Q)$$
$$+k'(\operatorname{Cot} i[\tan \phi'- \operatorname{Sec} \phi']- 1)] \quad (4.11)$$

$$\Delta\sigma_1-\Delta\sigma_3 = \tau_0[(1 + k'\operatorname{Cot} i)2 \operatorname{Sec} \phi'- Q \operatorname{Cot} i(1 - K_0)] \quad (4.12)$$

and $\Delta U = B[\Delta\sigma_3+ A(\Delta\sigma_1-\Delta\sigma_3)]$

$$= B\tau_0[\tan \phi'+(2A-1)\operatorname{Sec} \phi'+ \operatorname{Cot} i(1 -[K_0+A(1-K_0)]Q)$$
$$+k'(\operatorname{Cot} i[\tan \phi'+(2A-1) \operatorname{Sec} \phi'] - 1)]$$

$$(4.13)$$

substituting in equation 3.8 and rearranging terms,

$$k = \left(1- \frac{\rho_\omega}{\rho}\right)\frac{\tan\phi'-\tan i- B\tan\phi'[M\tan i + 1 -(K_0+ A[1-K_0])Q]}{1 + \tan\phi'\tan i + B \tan\phi'(M - \tan i)} \quad (4.14)$$

where

$M = \tan \phi'+ (2A - 1) \operatorname{Sec} \phi'$ $\quad\quad (4.15)$

i and ϕ' are the slope and internal friction angles
respectively,

ρ_ω and ρ are the mass densities of water and soil
respectively,

A and B are Skempton's pore pressure parameters,

$K = (1 - \operatorname{Sin} \phi)/(1 + \operatorname{Sin} i)$ $\quad\quad\quad\quad\quad$, and

$$Q = [(1 + K_0) - \sqrt{(1 + K_0)^2 - 4K_0 \, \text{Sec}^2 i}]/2K_0$$

Yield accelerations were calculated for various slope angles and various A and B parameters. Results are plotted in Fig. 4.5 along with the results obtained by Sarma's method.

On closer examination of these plots, it seems that the critical acceleration takes negative values as the slope angle approaches friction angle and for positive values of A parameter. However, as the initially mobilized friction angle ψ is always less than the internal friction angle ϕ', the reason for this unrealistic behaviour should extensively be incorporated in the pore pressure prediction. In other words, the excess pore pressure predicted by Skempton's equation is somewhat larger than the pore pressure required to get the effective stress circle into failure state.

To overcome the problem of negative critical accelerations, Pender introduced another new concept, a set of failure planes which are not parallel to the slope surface. However, if failure is not initiated on planes parallel to the slope surface, one more assumption was needed to construct the Mohr circle of stresses. Initially it was assumed that there is no change in the normal stress on planes perpendicular to the slope surface, due to the horizontal acceleration. Calculations were carried out for the case of no pore pressure response and an expression for the yield acceleration was obtained. Secondly, analysis was repeated by assuming that the centre of
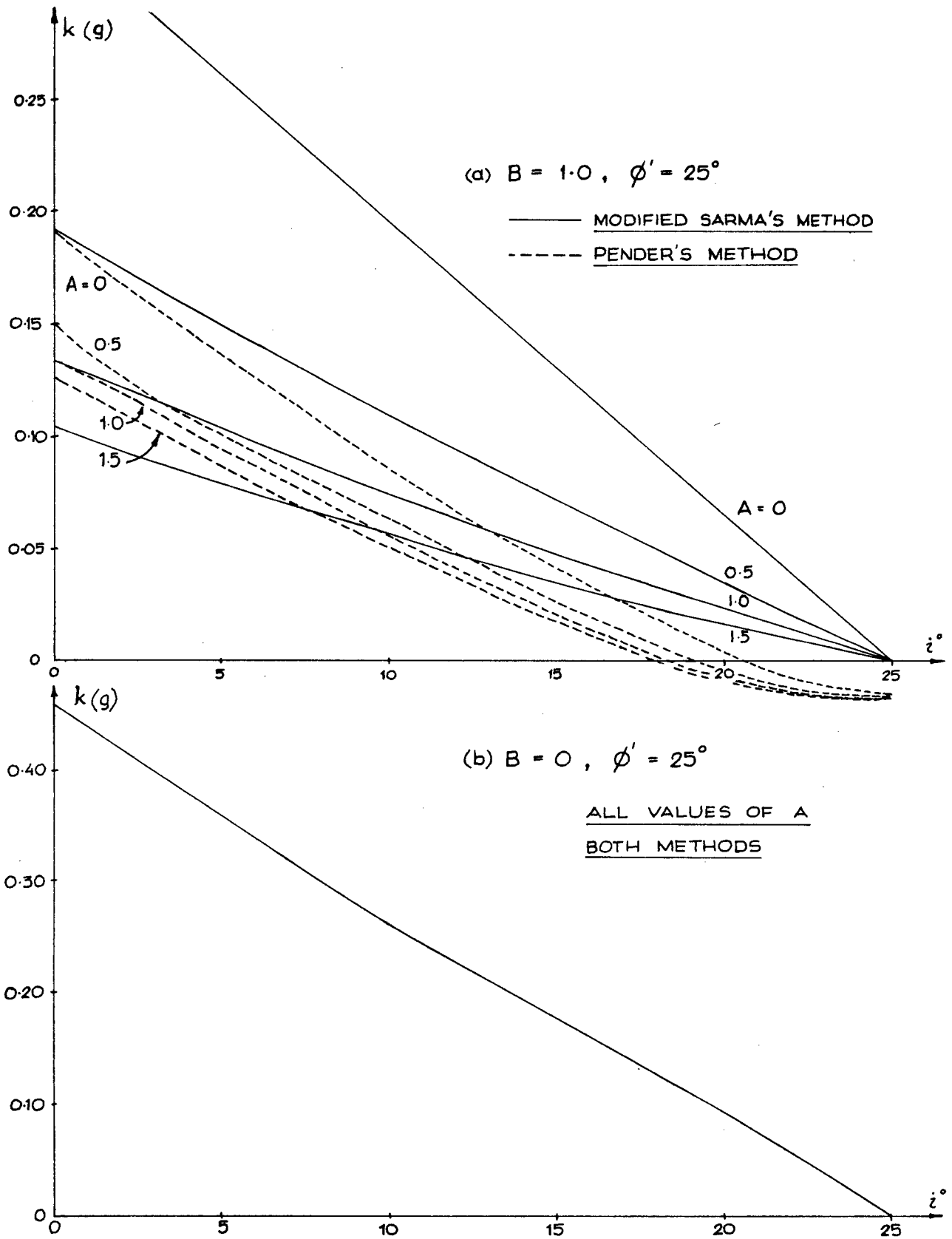
Fig.4.5 (a) Critical Accelerations for a Submerged
             Slope
         (b) Critical Accelerations for a Dry
             Slope

the total stress Mohr circle does not move due to the dynamic loading (Fig 4.6). Both the assumptions produced similar results and the second assumption was chosen as it seemed more likely and as it involved less tedious calculations.

A small change in notation is introduced here. Denote the normal stress on a plane parallel to the slope surface as σ'_{n1} and that on a plane perpendicular to the slope surface as σ'_{n2} , under in-situ stress conditions.

Now, referring to Figure 4.3 ($\sigma'_{n1} = \sigma'_{no}$ in the figure),

$$\sigma'_{n2} = \sigma'_{n1} - 2\tau_{max} \cos 2\beta \qquad (4.16)$$

where, $$\tau_{max} = 1/2(1 - K)\sigma'_{no} \qquad (4.17)$$

and $$K = (1 - \sin \phi')/(1 + \sin i) \qquad (4.18)$$

but $$\sigma'_{10} = Q\sigma'_{no} = Q\sigma'_{n1}$$

hence $$\sigma'_{n2} = \sigma'_{n1}[1 - (1 - K)Q \cos 2\beta] \qquad (4.19)$$

and $$\sin 2\beta = 2 \tan i/(1 - K)Q$$

hence $$\cos 2\beta = \sqrt{1 - 4 \tan^2 i/(1-K)^2 Q^2} \qquad (4.20)$$

or $$\sigma'_{n2} = \sigma'_{n1}[1 - \sqrt{(1-K)^2 Q^2 - 4 \tan^2 i}]$$

if $$P = 1 - \sqrt{(1-K)^2 Q^2 - 4 \tan^2 i}, \qquad (4.21)$$

$$\sigma' = P\sigma'_1$$

(a) *Total / Effective Stress Mohr Circle for initial Conditions ($U_o = 0$)*
(b) *Total Stress Mohr Circle after the application of Inertia Force*
(c) *Effective Stress Mohr Circle after the application of Inertia Force*
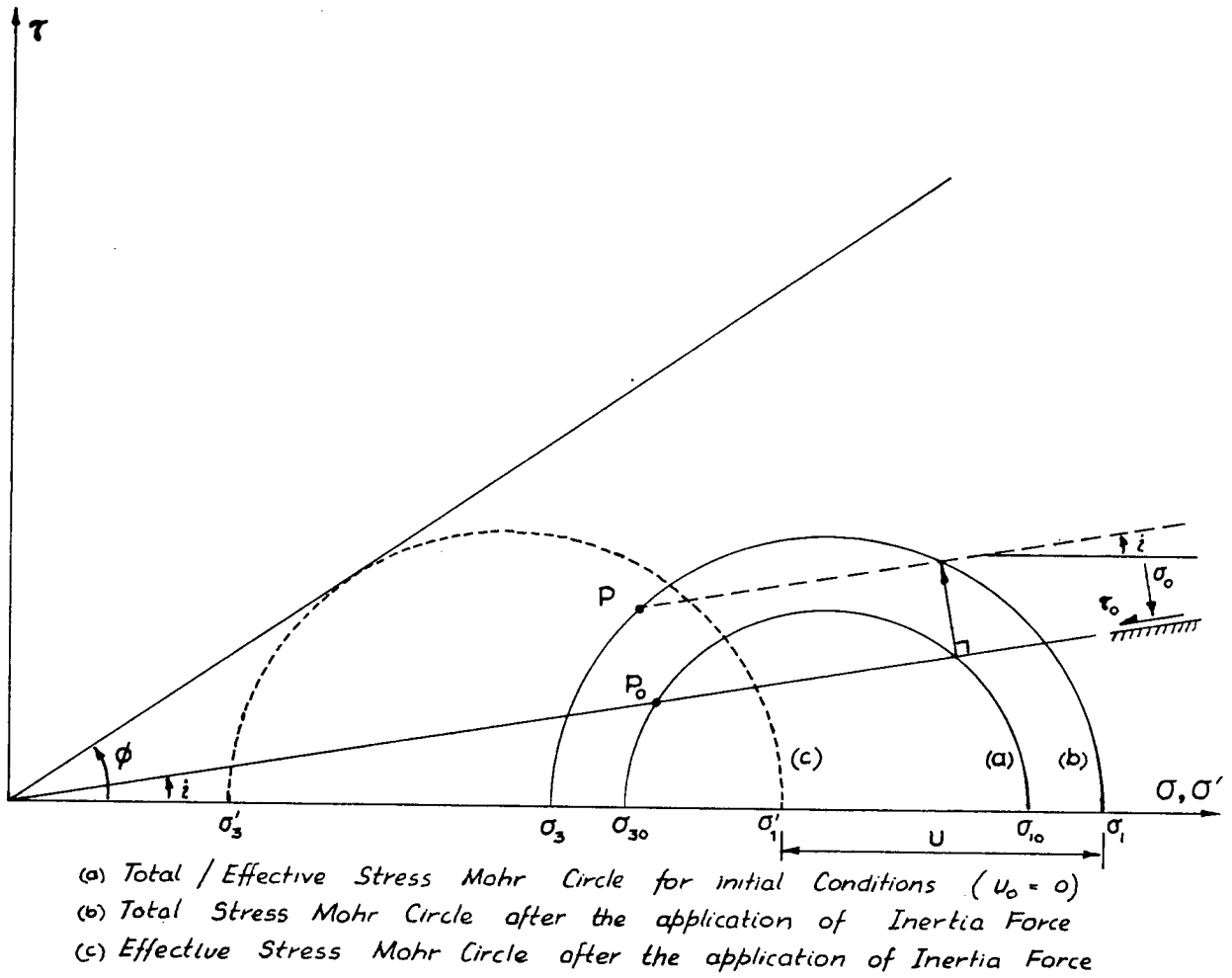
Fig.4.6   Concept of Failure Planes which are
          not Parallal to the Slope Surface

Now, after the introduction of earthquake inertia force kg,

$$\tau = \sigma'_{n1}(k' + \tan i)$$
$$\sigma = \sigma'_{n1}(1 - k'\tan i) \qquad (4.22)$$

Assuming that the centre of the total stress Mohr circle does not move due to the dynamic loading,

$$1/2(\sigma_1+\sigma_3) = 1/2(\sigma'_{n1}+\sigma'_{n2}) = 1/2(1 + P)\sigma'_{n1} \qquad (4.23)$$

for no initial excess pore water pressure.
and so,

$$1/2(\sigma_1-\sigma_3) = \sigma'_{n1}\sqrt{(k'+\tan i)^2+[(1-k'\tan i)-1/2(1+P)]^2}$$
$$= \sigma'_{n1}\sqrt{k'^2(1+\tan^2 i)+k'\tan i(1+P)+(\tan^2 i+1/4(1+P)^2-P)} \qquad (4.24)$$

principal stress changes are related by,

$$\Delta\sigma_3= - \Delta\sigma_1 \qquad (4.25)$$

and hence, the pore water pressure change

$$\Delta U = B (2A - 1) \Delta\sigma_1 \qquad (4.26)$$

but $\Delta\sigma_1= 1/2(\sigma_1-\sigma_3) - 1/2(\sigma_{10} -\sigma_{30})$

$$= \sigma'_{n1}[\sqrt{k'^2(1+\tan^2 i)+k'\tan i(1+P)+(\tan^2 i+1/4(1+P)^2-P)}$$
$$-\sqrt{1/4(1-P)^2 + \tan^2 i}]$$

now, at the initiation of failure,

$$\sin \phi' = \frac{1/2(\sigma'_1-\sigma'_3)}{1/2(\sigma'_1+\sigma'_3)} = \frac{1/2(\sigma_1-\sigma_3)}{1/2(\sigma_1+\sigma_3)-\Delta U} \qquad (4.27)$$

substituting from equations 4.22, 4.23 and 4.24 and rearranging terms,

$$k'^2 \sec^2 i + k'\tan i(1+P) + [\tan^2 i +\sqrt{1/4(1-P)^2-N^2}] = 0$$

hence, the yield acceleration will be given by,

$$k' = [-\bar{B} - \sqrt{\bar{B}^2 - 4\bar{A}\bar{C}}] / 2\bar{A} \qquad (4.28)$$

where, $k' = k /(1 - \rho_\omega/\rho)$

$\bar{A} = \sec^2 i$

$\bar{B} = \tan i (1 + P)$

$\bar{C} = \tan^2 i+\sqrt{1/4(1-P)^2-N^2}$

$P = 1 - \sqrt{(1-K)^2 Q^2 - 4\tan^2 i}$

$Q = [(1+K_0)-\sqrt{(1+K_0)^2-4K_0\sec^2 i}] / 2K_0$ and

$$N = \frac{1/2(1+P) + B(2A-1)\sqrt{1/4(1-P)^2 + \tan^2 i}}{\text{Cosec } \phi' + B(2A-1)} \qquad (4.29)$$

Critical acceleration values calculated by equation 4.27 are much lower than the values given by modified Sarma's

method (Fig. 4.7). The effect of these differences on
displacement calculations and the validity of the preceeding
analysis will be discussed in the next chapter.
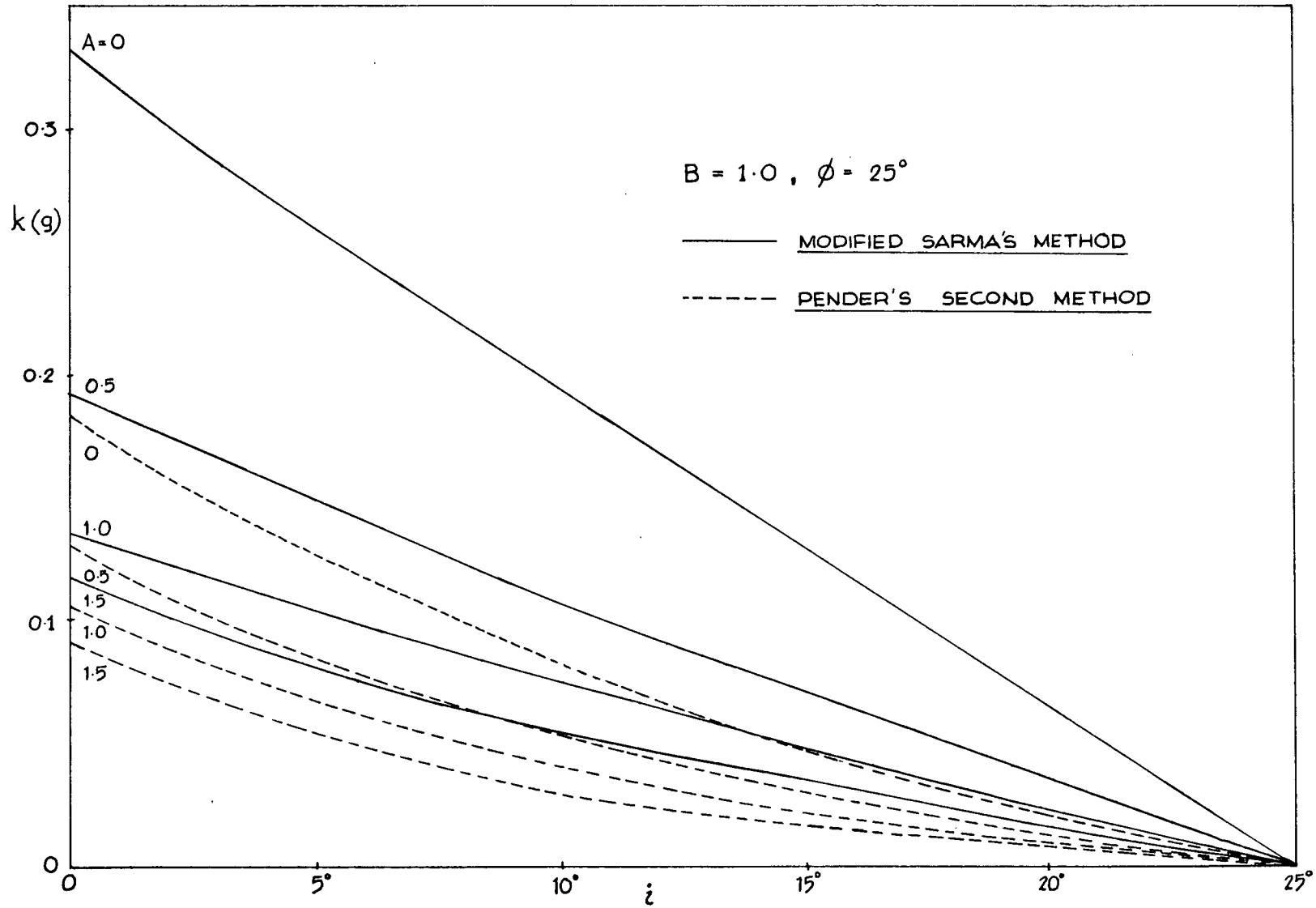
Fig.4.7 Comparison of Critical Accelerations
by Sarma's and Pender's Second Method

CHAPTER 5

COMPARISON OF PSEUDO-STATIC METHODS.

5.1 General.

Three pseudo-static methods of analysing underwater slopes were discussed and expressions were presented to calculate the yield acceleration. Modified Sarma's method and Pender's first method degenerates to Seed and Goodman's expression for dry soils when the corresponding soil parameters are included. Pender's second method, however, results in a different expression under the dry, on-shore conditions.

Pender's first method resulted in negative critical accelerations for slope angles approaching the internal friction angle of the soil. Although the slopes generally encountered in most of the offshore sites are rather small, higher slopes are not unlikely. Thus, it is reasonable to avoid using Pender's first method in calculating critical acceleration.

The yield accelerations calculated by Pender's second method are considerably smaller than the values obtained by

modified Sarma's method, but not unrealistic. However, the
differences in critical accelerations will be greately
reflected in displacement calculations.

5.2 Displacement Calculations.

Earthquake induced displacements are generally
calculated by double integrating the acceleration in excess of
the yield acceleration. For a single acceleration pulse of
magnitude Ag, and a duration t_0, it was shown in Chapter 2,
that the displacement will be given by,

$$u_m = \frac{V^2}{2gk} \left(1 - \frac{k}{A}\right) \qquad (5.1)$$

where, k is the critical acceleration, and

V is the maximum ground velocity = Agt_0.

In the actual situation or in using a design
acceleration history, the earthquake record consists of a
number of such pulses of different magnitudes and different
signs. The design acceleration history is usually converted to
pulses of the same duration, to make the manipulation less
difficult.

As long as the ground acceleration is lower than the
critical acceleration, there will not be any movement of the
ground. Once the ground acceleration exceeds the yield, a

positive velocity and a corresponding positive displacement will result. When the ground acceleration drops below yield, velocity will start decreasing. Nevertheless, displacement continues to increase in the positive direction until the ground comes to rest.i.e., until the velocity becomes zero. This is illustrated in Fig. 5.1. A computer programme was written to calculate the displacements and velocities corresponding to a given acceleration record, which is documented in the Appendix. This programme is capable of calculating the critical acceleration, and carrying out the complete analysis following the specified method.

5.3 Comparison of rigid body analysis methods.

The previously discussed rigid body analysis methods were compared by applying these methods to analyse the same slope under the same acceleration history. For this comparison, a normally consolidated clay slope was selected and an internal friction angle of 25^0 and a slope angle of 10^0 was assumed. The first 10 seconds of El Centro (1940) acceleration record (N - S component) was used as the input motion after scaling it down to a maximum acceleration of 0.3g, and displacements were calculated by all three methods. Results are tabulated in Table 2 for varying pore pressure parameters.

It can easily be seen from the table that the displacements calculated by Pender's second method are much
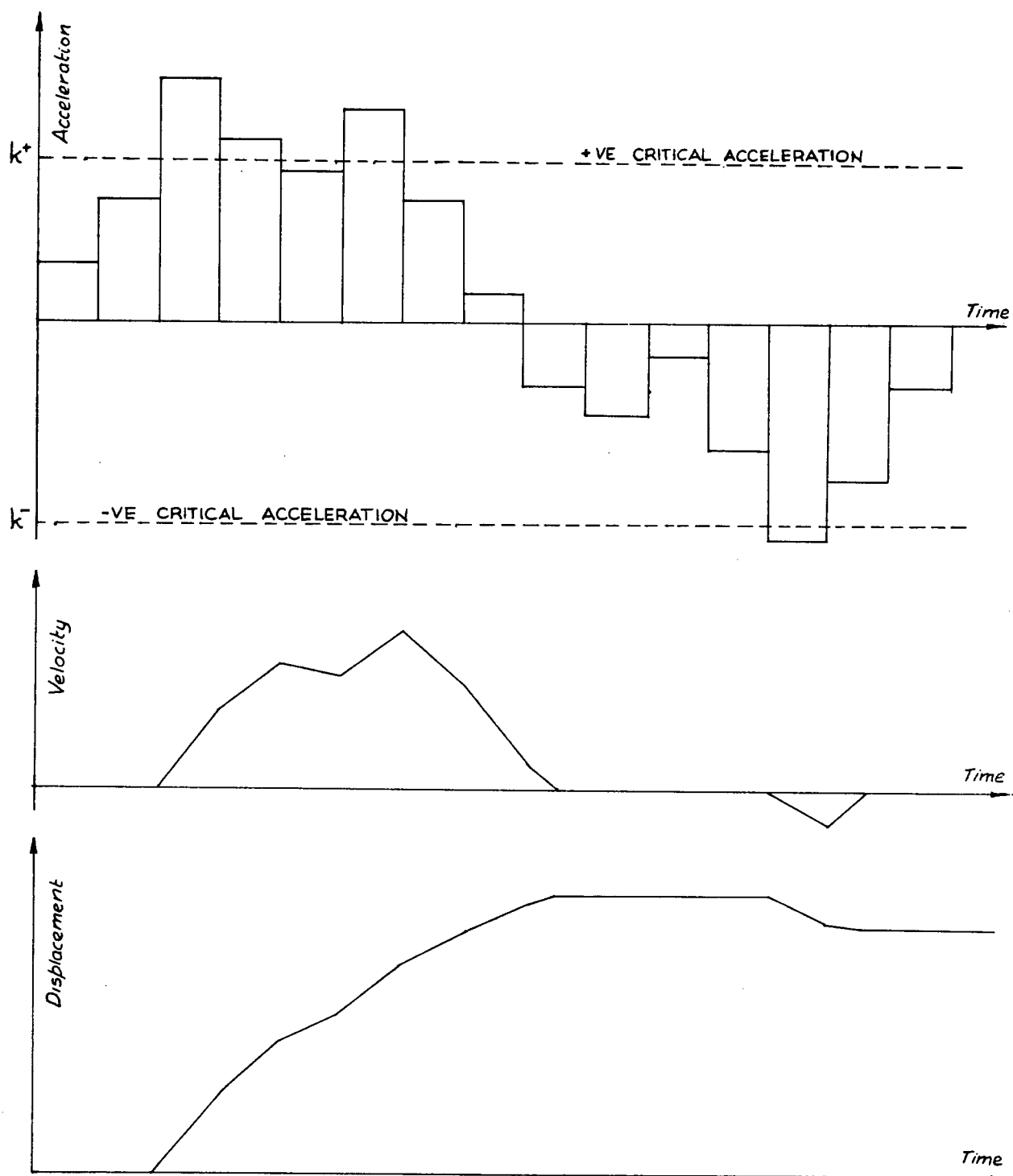
Fig.5.1 Calculation of Displacements due to a
given Acceleration History

TABLE 2

CRITICAL ACCELERATIONS AND CORRESPONDING DISPLACEMENTS

Earthquake input - First 10 seconds of El Centro (1940)

earthquake, N - S component.

Internal friction angle of the soil is 25°

A and B are Skempton's pore pressure parameters.

(a) Dry soil, B = 0.

	Crit. Accn.(g)			Displacement (in)		
	A=0	A=0.5	A=1	A=0	A=0.5	A=1
Seed and Goodman's Method	0.268	0.268	0.268	.0002	.0002	.0002
Modified Sarma's Method	0.268	0.268	0.268	.0002	.0002	.0002
Pender's Second Method	0.103	0.103	0.103	0.380	0.380	0.380

TABLE 2 (Cont'd)

(b) Partially Saturated Soil, B = 0.5.

	Crit. Accn.(g)			Displacement (in)		
	A=0	A=0.5	A=1	A=0	A=0.5	A=1
Modified Sarma's Method	0.158	0.121	0.098	0.063	0.184	0.470
Pender's Second Method	0.063	0.051	0.043	2.271	4.101	7.540

(c) Saturated Soil, B = 1.0.

	Crit. Accn.(g)			Displacement (in)		
	A=0	A=0.5	A=1	A=0	A=0.5	A=1
Modified Sarma's Method	0.195	0.109	0.075	0.017	0.288	1.253
Pender's Second Method	0.084	0.051	0.038	0.862	4.101	11.23

higher than those calculated by the other two methods. This is to be expected with a very low value of yield acceleration. However, as these displacements are extremely large and hence unrealistic, the validity of Pender's second method has to be considered carefully.

5.4 Validity of Pender's Second Method.

Pender's second method is based on two major hypotheses. First hypothesis, the assumption on the principal stress ratio, was brought up for the purpose of drawing the initial Mohr circle. Mobilized friction angles resulted by the use of this hypothesis are reasonable and the assumed equation degenerates to known forms under some special conditions.

The second hypothesis, a failure plane which is not parallel to the slope surface, is questionable as it is contradictory to the most obvious failure, parallel to the slope surface. However, Pender (1982) argiues that although the failure initiates on a different plane, it eventually becomes parallel to the slope surface. The displacement calculations were carried out, based on this statement. This kind of plane rotation, according to Pender (1982), is discussed by de Josselin de Jong (1971) and Randolph and Wroth (1981). However, the present problem is not comparable to the cases described by these authors, on the following grounds.

(a) Randolph and Wroth (1981) analyses the failure mechanism with regard to simple shear apparatus. Experimental and theoretical evidences are mentioned in support of coincidence of rupture planes and zero extension planes. But when a slope is failing as a rigid body, it is hard to define a zero extension plane.

(b) In Pender's model, initiation of failure is on a plane of maximum stress obliquity ($\tan \phi' = \tau/\sigma'$), and then it rotates to a plane with lesser stress obliquity. Randolph and Wroth (1981) discuss a stress rotation TO the plane of maximum stress obliquity and not FROM such a plane.

(c) De Josselin de Jong (1971) has pointed out that, the soil might choose the most convenient mode of failure (i.e.,that which requires the lowest external applied load). Hence if the most obvious mode of failure is along a plane parallel to the slope surface, the question arises, why does it initiate on a different plane ?.

Hence it is obvious that the drawbacks in Pender's second method are outweighing the single drawback in modified Sarma's method, the higher principal stress rotation. It can then be concluded that, among the rigid body analysis procedures considered, modified Sarma's method is the most suitable one to use in practice. This conclusion has to be

verified by comparing the results of the rigid body analysis method against those of more complex, non linear effective stress analysis procedures.

CHAPTER 6

COMPARISON OF RESPONSE DATA FROM RIGID BODY AND COMPLIANT

MODELS.

6.1 Introduction.

In geotechnical engineering, verification of a new
model is usually done by comparing the results with measured
values in the field. For the particular problem of deformations
in offshore slopes, it is extremely difficult to find field
data for comparison. Until such data are available, it is
worthwhile to compare previously discussed rigid body analysis
methods with more complex, nonlinear effective stress analysis
procedures.

As discussed in Chapter 2, several computer
programmes are available for carrying out a dynamic analysis on
horizontal soil layers. True non linear programmes are becoming
popular and are believed to yield results more representative
of field behaviour than previously developed programmes based
on the equivalent linear approach. For the comparison which
will be discussed herein, the true non linear computer
programme DONAL-2 has been used.

Section 6.2 deals with the comparisons of DONAL-2 with the other available methods. Comparisons with rigid body methods are discussed in Sections 6.2.1 and 6.2.2. The other available non-linear programme DCHARMS is compared with DONAL-2 in the analysis reported in Section 6.2.3.

Conclusions of this Chapter are included in Section 6.3.

6.2 Comparison Procedures.

6.2.1 Seed and Goodman's method

Seed and Goodman (1964) introduced a method for calculating the yield accelerations, and subsequently the displacements, for slopes composed of dry sand. The equation for yield acceleration has later been modified to include the effect of a shear strength intercept, S_i . As the method can now handle materials with both cohesion and internal friction, it can be compared with DONAL-2, using the first option (dynamic response only).

Two types of acceleration records were used for comparison. First 10 seconds of El Centro (1940) earthquake record and a sinusoidal acceleration input were used in almost all example runs. The sinusoidal acceleration record, generated for this purpose, is shown in Figure 6.1. Two seconds of quiet

period was added at the end of the record in both cases.

A dry sand slope of 15° was analysed first, using the two different methods. The slope was represented for the DONAL analysis by six sloping layers, each 4 ft thick, resting on a rigid base. A friction angle of 35° was assumed for the sand. Maximum acceleration used is 0.45g for both types of input motions. Results are given below in the form of residual deformations.

(1) El Centro earhquake, N-S component

    Seed and Goodman's Method   0.005 ft
    DONAL 2   0.941 ft

(2) Sinusoidal input

    Seed and Goodman's Method   0.102 ft
    DONAL 2   2.546 ft

It is clear that there is a vast difference in the two methods of calculating residual deformations. Seed and Goodman's method, when used to analyse a slope made of a material having only the frictional resistance, does not define a failure surface. In doing their shaking table experiments, Seed and Goodman defined the yield acceleration as the acceleration at which sand grains on the top layer start to move downslope. This movement was observed by using coloured sand particles and a telescope. In DONAL-2 programme, earthquake acceleration is transmitted to the slope at the base, 24 feet below the surface in previous example, and hence,
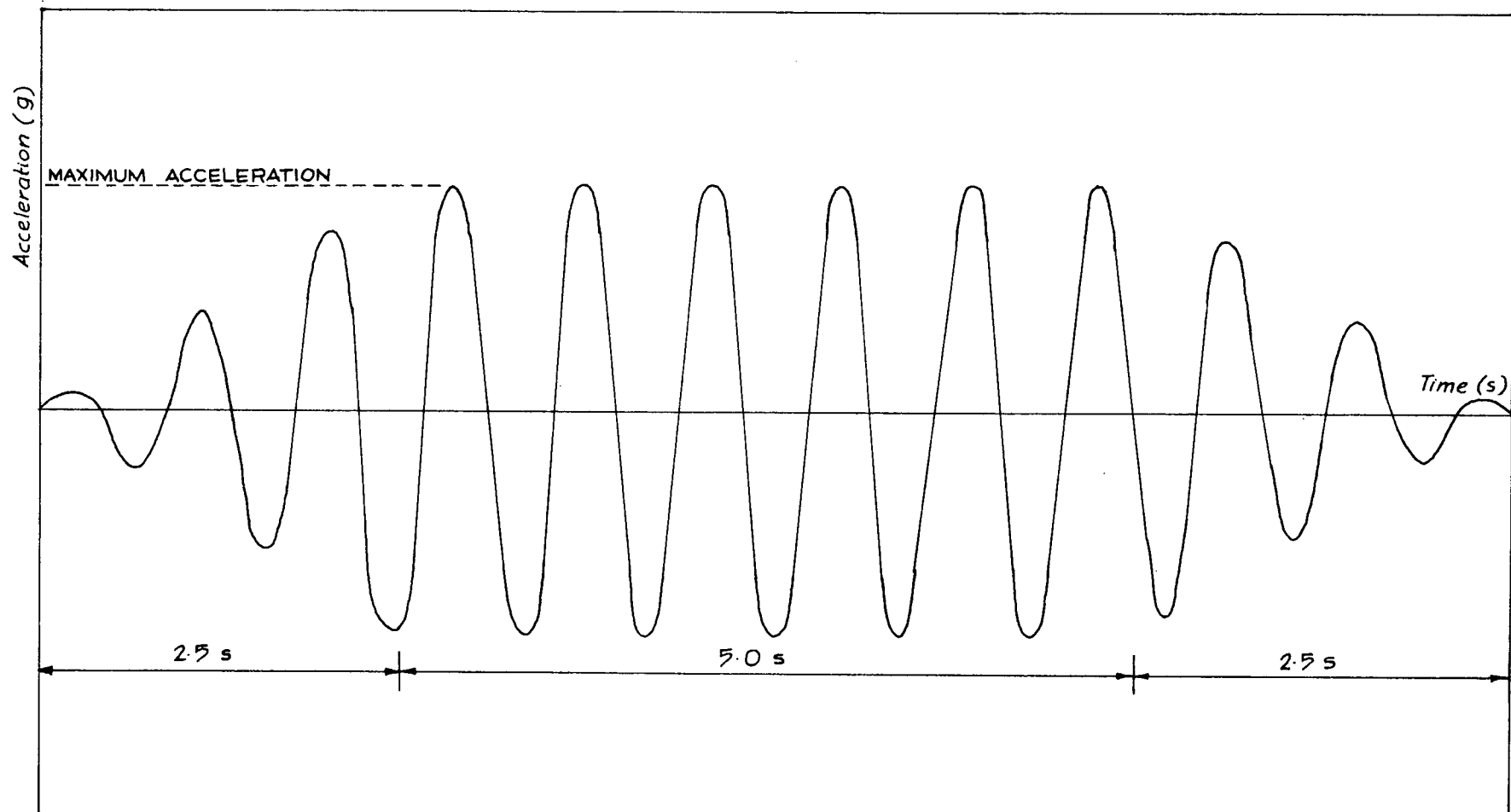
Fig.6.1   Sinusoidal Acceleration Record used as
          the Input

amplification of input motion takes place throughout the
deposit. Deformation occurs at each and every point in the soil
mass and a very large relative displacement is seen at the
slope surface.

It is evident from the aforementioned reasoning that
the comparison of the two methods of analysis is not of any
value in the case of slopes composed of materials having only
the frictional resistance. Hence it is decided to see the
effect of a shear strength intercept on the earthquake induced
deformations. Seed and Goodman's original equation for yield
acceleration (eq. 2.7) will not be valid for this analysis and
it can be shown that the new equation for yield acceleration
for an infinite slope is

$$k \ = \ \tan \ (\phi' \ - \ i \ ) \ + \ \frac{S_i}{d \gamma \ (\text{Cos } i \ + \ \text{Sin } i \ \tan \ \phi')} \quad (6.1)$$

where S_i = shear strength intercept,

d = depth of sliding surface,

γ = unit weight of soil   and

ϕ' and i have their usual definitions

This expression has the depth d as a variable and
hence the two types of analysis were carried out for varying
depth of sliding surface. In DONAL runs, earthquake input was
applied at the bottom of the soil mass considered .i.e. at the
depth d. In defining non-linear stress strain curve for the

soil, it was necessary to modify the equation for τ_{ult} , taking shear strength intercept into account.

From DESRA-2 (Lee and Finn, 1978), the equation for ultimate shear stress τ_{ult} , to use in hyperbolic stress-strain relation is,

$$\tau = \left\{ \left(\frac{1 + K_0}{2} \sin \phi \right)^2 - \left(\frac{1 - K_0}{2} \right)^2 \right\}^{1/2} \sigma'_{vo} \qquad (6.2)$$

This expresion is developed by the use of a Mohr circle, and by assuming K conditions at rest for a horizontal sand deposit. For a clayey soil, however, a modification of this equation is required in order to include the effect of cohesion intercept.

According to Figure 6.2, the ultimate shear stress is given by AB.
Hence,

$$\tau = \left\{ \left[\left(\frac{1 + K_0}{2} \right) \sigma'_{vo} \sin \phi + c \cos \phi \right]^2 - \left(\frac{1 - K_0}{2} \right)^2 \sigma'^2_{vo} \right\}^{1/2} \qquad (6.3)$$

The same slope (slope angle = 15°, friction angle = 35°) was analysed again with a shear strength intercept of 100 psf. Residual deformations given by the two methods are tabulated in Table 3(a). The differences between the two methods are still considerably large. As in the previous case, there still is a very high amplification in the input
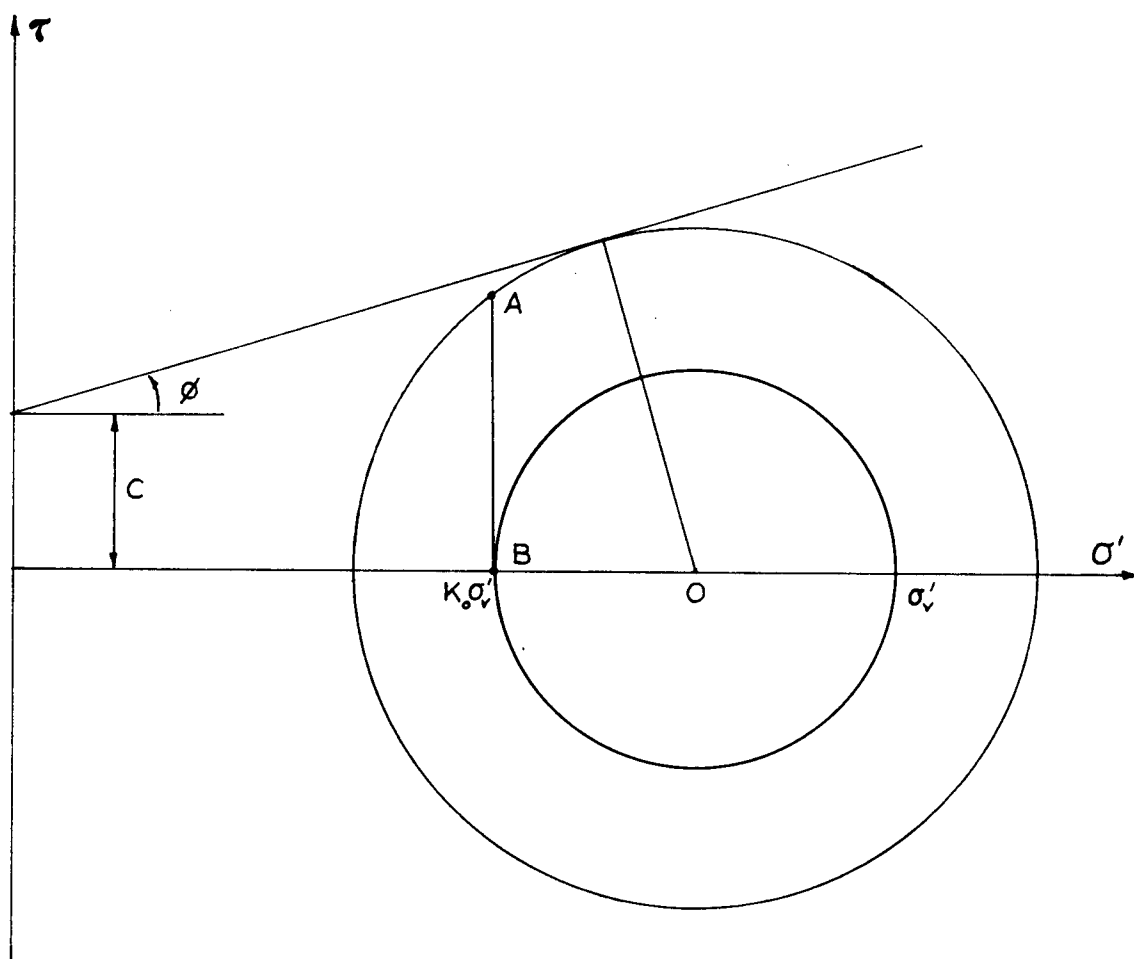
Fig.6.2 Calculation of Ultimate Shear Stress
for a C – φ Material

acceleration when coming from the bottom of the deposit to the slope surface, when using a non-linear programme. Rigid body method of analysis, however, has the same acceleration, the input, throughout the deposit.

As the last step of comparison between Seed and Goodman type of analysis with DONAL-2, it was decided to choose a material with no frictional resistance and only a shear strength intercept (similar to cohesion). The equation for yield acceleration now reduces to

$$k = \text{Sec } i \ (\ c/d\gamma \ - \ \text{Sin } i \ ) \qquad\qquad (6.4)$$

This expression breaks down for relatively higher depths as $c/d\gamma$ drops below Sin i. For example, if $\gamma = 114$ pcf and if $c = S_i = 100$ psf, static failure occurs for depths higher than 12.57 feet in a 4° slope. On the other hand, when the depth is too small, yield acceleration becomes very high and as a result, Seed and Goodman's method predicts no displacements. Because of these two reasons comparison is possible only for some intermediate depths of sliding surface.

A cohesive slope of 4° was selected for the analysis and first 15 seconds of S-E component of Imperial valley earthquake record was used as the input. Maximum acceleration was scaled down to 0.145g and a cohesion intercept of 150 psf was used. Results of this analysis are given in Table 3(b) for two depths of sliding surface. Table 3(c) presents residual

TABLE 3

RESIDUAL DEFORMATIONS DUE TO DYNAMIC LOADING

(a) Sinusoidal input with a_{max} = 0.45g, Period = 0.25s

Duration = 12s

Shear Strength Intercept = 100 psf

Friction angle = 35°

Slope angle = 15°

Depth of Sliding Surface (ft)	Residual Deformation (ft)	
	Seed and Goodman's Method	DONAL-2 Program
4	0.000	0.107
8	0.000	0.488
12	0.008	0.987
16	0.021	1.516
20	0.032	1.987
24	0.041	2.346

TABLE 3 (Cont'd)

(b) Imperial valley earthquake, S - E Component with

a_{max} = 0.145g,   slope = 4^0

duration = 15 s,   cohesion = 150 psf

Depth of Sliding Surface(ft)	Residual Deformation (ft)	
	Seed and Goodman's Method	DONAL-2 Program
10	0.057	0.030
15	2.320	0.081

(c) Sinusoidal input with a_{max} = 0.15g,   slope = 4^0

duration = 12 s,   cohesion = 150 psf

Depth of Sliding Surface (ft)	Residual Deformation (ft)	
	Seed and Goodman's Method	DONAL-2 Program
10	0.262	0.019
15	44.900	0.025

deformations of the same slope with a sinusoidal acceleration
input.

It is clear from the results that comparable
displacements are obtained only for the sliding surface depth
of 10 feet (Table 3(b)), for which case the total build up of
the displacement is plotted in Figure 6.3.

6.2.2 Modified Sarma's method

Sarma (1975), used Skempton's pore pressure
parameters to calculate the pore pressure increase in a slope
due to earthquake shaking. This method has been modified as was
explained in Chapter 3, for offshore slopes. The analysis was
based on a limit equilibrium principle and obeys the Mohr-
Coulomb failure criteria with effective stresses. In the
analysis described earlier, expressions have been derived only
for a cohesionless material. However, the same analysis can
easily be carried out for a material with both the cohesion and
internal friction as will be discussed later in this chapter.

The major difference in Sarma's method and Seed and
Goodman's method is the incorporation of pore water pressure.
Material properties and the amount of saturation can be taken
into account by Skempton's pore pressure parameters. An on
shore slope made out of cohesionless material was chosen first,
to compare with the DONAL programme. Pore pressure parameters A
and B were varied and the same two acceleration records, as in
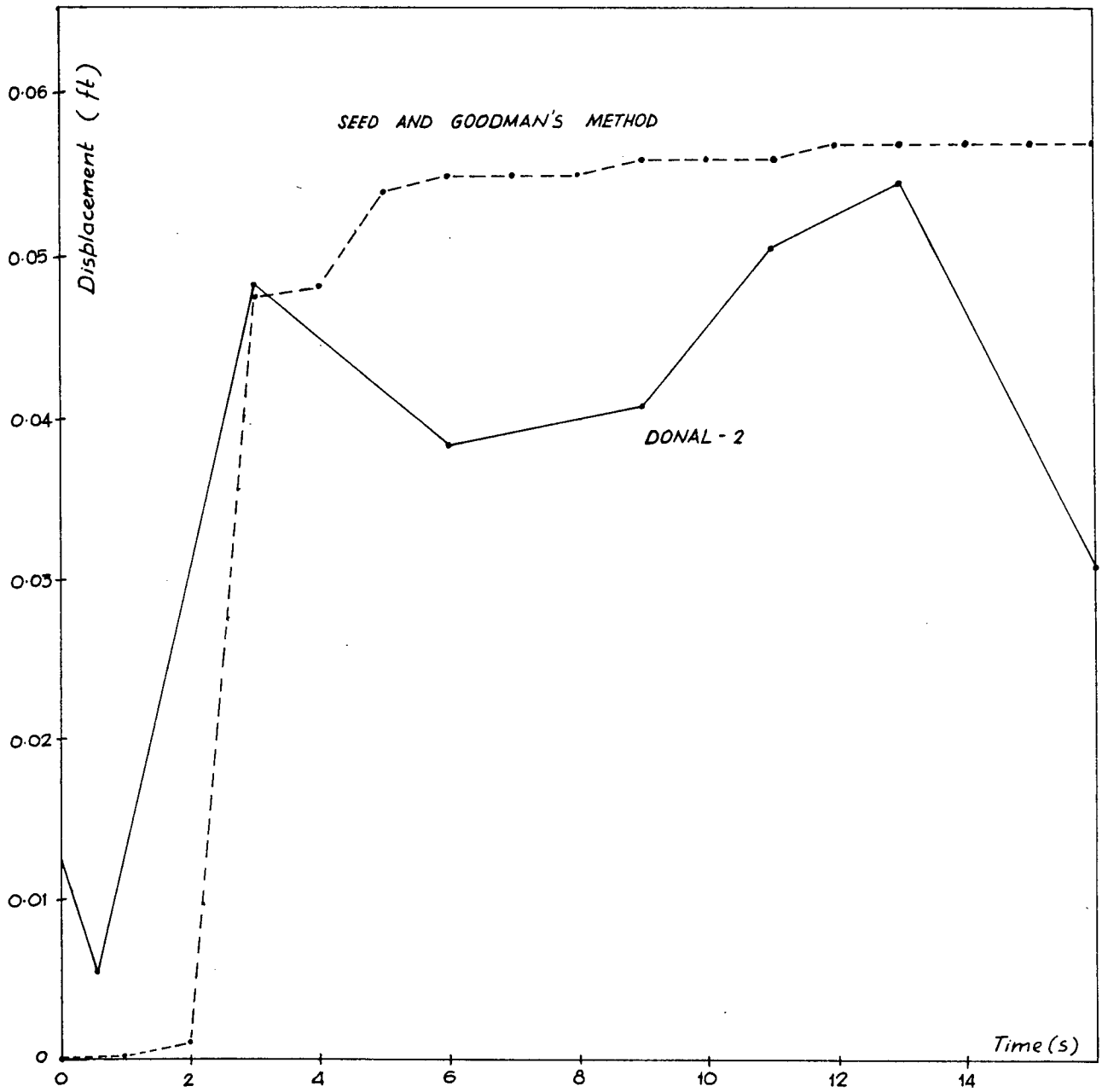
Fig.6.3   Residual Deformations in a Cohesive Slope

the previous case, were used as the input motions. Results are tabulated in Table 4, for a 15° slope. Maximum acceleration used was 0.45g and results are given for both types of input motions.

The following conclusions can immediately be made by observing these results.

(1) Final displacement of the slope is greatly dependent on the values of pore pressure parameters.

(2) For constant A or B, final displacement increases with increasing B or A respectively (with the exception of the case B = 0.0).

In modified Sarma's method, yield acceleration is different for a saturated slope from that for a submerged slope. In non-linear analysis, pore pressure calculations can be made only in the layers which are submerged. Hence it is impossible to compare the displacements in a saturated slope.

At this stage, it is worthwhile to compare the displacements of a submerged slope as that option is available in the DONAL programme. Same example problem was analysed, but with a 5° slope to match usual offshore gradients and with all layers submerged, and following values of residual deformations are given by non linear analysis.

El Centro earthquake, N - S component   0.102 ft

Sinusoidal input   0.433 ft

For a submerged slope, Skempton's B is 1.0 and as for

TABLE 4

RESIDUAL DEFORMATIONS BY MODIFIED SARMA'S METHOD

(a) El Centro Earthquake, N - S component with

$$a_{max} = 0.45g$$

Duration = 12s

Friction angle = 35°

Slope angle = 15°

Residual Deformation (ft)			
Skempton's A Parameter	Skempton's B Parameter		
	0.0	0.5	1.0
0.0	0.005	0.0	0.0
0.5	0.005	0.027	0.106
1.0	0.005	0.176	1.198

TABLE 4 (Cont'd)

(b) Sinusoidal input with

$$a_{max} = 0.45g$$

$$\text{Duration} = 12s$$

$$\text{Friction angle} = 35^\circ$$

$$\text{Slope angle} = 15^\circ$$

	Residual Deformation (ft)		
Skempton's A Parameter	Skempton's B Parameter		
	0.0	0.5	1.0
0.0	0.102	0.0	0.0
0.5	0.102	0.370	0.789
1.0	0.102	1.072	23.67

sea bottom soft sediments Skempton's A is positive, a A value of 0.35 was chosen. Residual deformations calculated by using modified Sarma's method are given below for the two types of input motioons.

El Centro earthquake, N - S component   0.125 ft

Sinusoidal input   0.867 ft

It is clear from these results that the comparison is much better than was observed in the comparison with Seed and Goodman's method. To complete the analysis, same procedure was followed for a submerged clay slope. A clay slope with a 50 psf cohesion intercept and 5° slope angle was selected as the example problem and a friction angle of 25° was assumed. By following the analysis described in Chapter 3 for a material with both cohesion and internal friction, the following expression was emerged for critical acceleration.

$$k' = \frac{\tan\phi - D\tan i - B\tan i\tan\phi[\tan\phi - \tan\psi_0 - (1-2A)(\text{Sec}\phi - \text{Sec}\psi_0)]}{1 + \tan i\tan\phi + B\tan\phi[\tan\phi - \tan i - (1-2A)\text{Sec}\phi]} \quad (6.5)$$

where $D = 1 - c/\tau_0$ (6.6)

Rigid body type analysis was carried out using modified Sarma's method for a sliding surface depth of 24 feet and following final displacements have been obtained for the two types of input motions.

El Centro earthquake, N - S component   0.35 ft

Sinusoidal input   2.27 ft

Analysis was repeated by using non-linear programme DONAL-2 and corresponding residual deformations are given below.

El Centro earthquake, N - S component   3.66 ft
Sinusoidal input   2.88 ft

6.2.3 Degradation of Clay.

When a sand sample is loaded, either statically or dynamically, pore water pressures are generated, reducing the effective stress. This loss in strength leads to cyclic mobility and may eventually result in liquefaction of sand. In offshore, however, sand layers are rarely in existance. Many marine deposits are soft clay layers. These clays exhibit a phenomenon called modulus degradation under repeated loading. Degradation is associated with an increase in pore water pressure during cyclic loading and also with deterioration of the structure of clay due to remoulding. Hence, one cannot overlook the importance of degradation in designing an offshore structure located at a soft clay site.

A clay slope can be analysed with the inclusion of the effect of degradation by using the available computer programmes, DONAL-2 and DCHARMS. However, it is important to note that there are three main differences in these two methods as discussed in Chapter 2.

(1) DONAL-2 uses a hyperbolic stress-strain relationship and DCHARMS uses a Ramberg-Osgood type constitutive relation.

(2) The form of the relationship between degradation parameter t and the cyclic shear stress level, is different in the two programmes.

(3) DONAL-2 calculates the displacement by direct integration of the dynamical differential equation. DCHARMS assumes a unique relationship between residual shear strain in the downslope direction and the degradation index δ.

It was decided to compare the two programmes by applying them to analyse an example problem. The example problem used by Moriwaki et al. (1982) was selected and the hypothetical soil profile is given in Table 5.

The same soil profile was analysed by DONAL-2 in its 4th option. However, G_{max} has to be changed to match the backbone curves (Ramberg- Osgood and hyperbolic) at expected strain levels. Taft, 1952 Kern County earthquake, S69E component was used as the input motion at the base with maximum acceleration scaled to 0.33g. Residual displacements are plotted against time in Figure 6.4.

Figure 6.5 shows the relationship between degradation parameter t and cyclic strain, as used in the example run. It can be seen by Fig 6.6 that the two backbone curves are

TABLE 5

SOIL PROFILE USED IN EXAMPLE RUN.

Layer No.	Thikness-ft	G-ksf	Soil Type
1	4.9	200.0	Soft Clay
2	4.9	202.9	Soft Clay
3	5.6	266.1	Soft Clay
4	6.9	401.8	Soft Clay
5	8.1	558.2	Soft Clay
6	9.3	737.6	Soft Clay
7	10.5	961.2	Soft Clay
8	22.5	4224.0	Stiff Clay
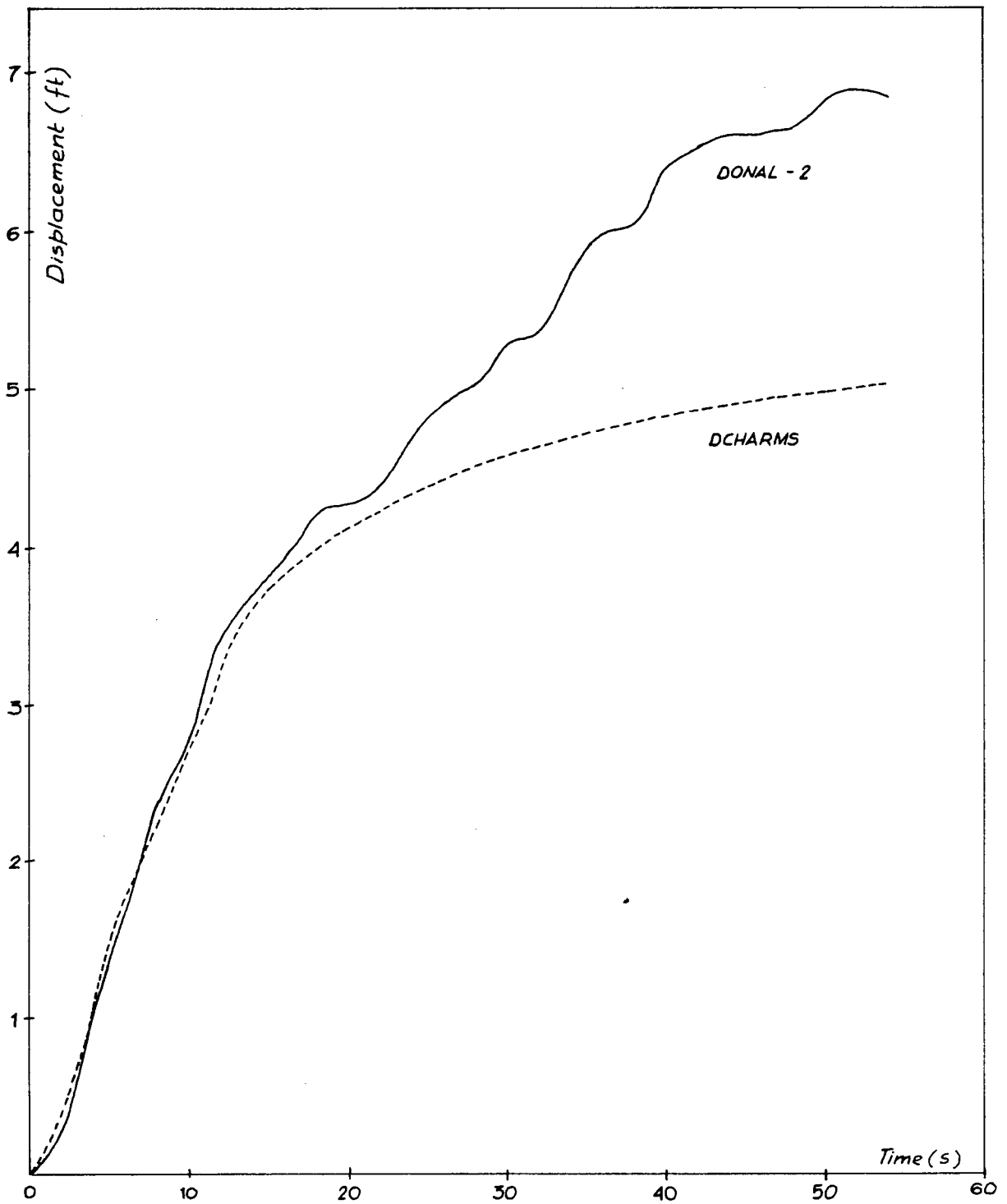
Fig.6.4   Displacement Patterns by using Non-Linear
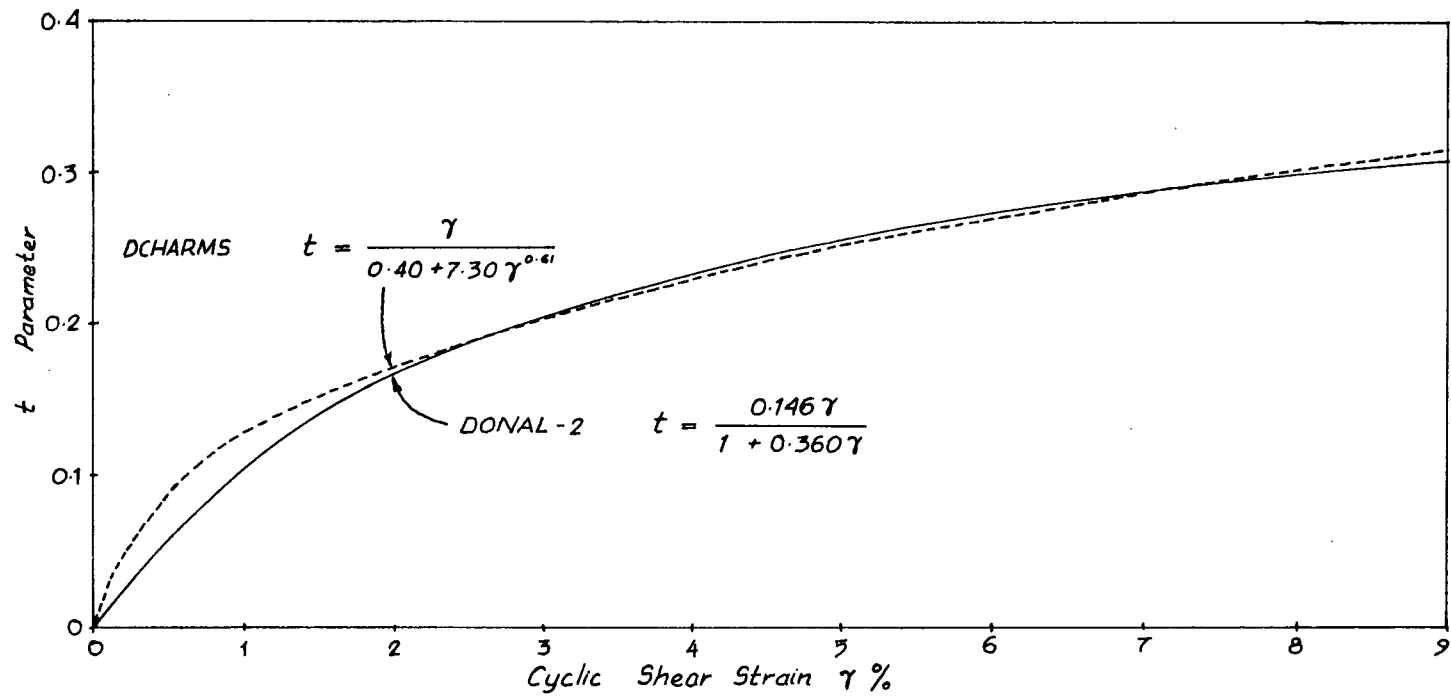   Programmes

Fig.6.5   Relationship Between degradation
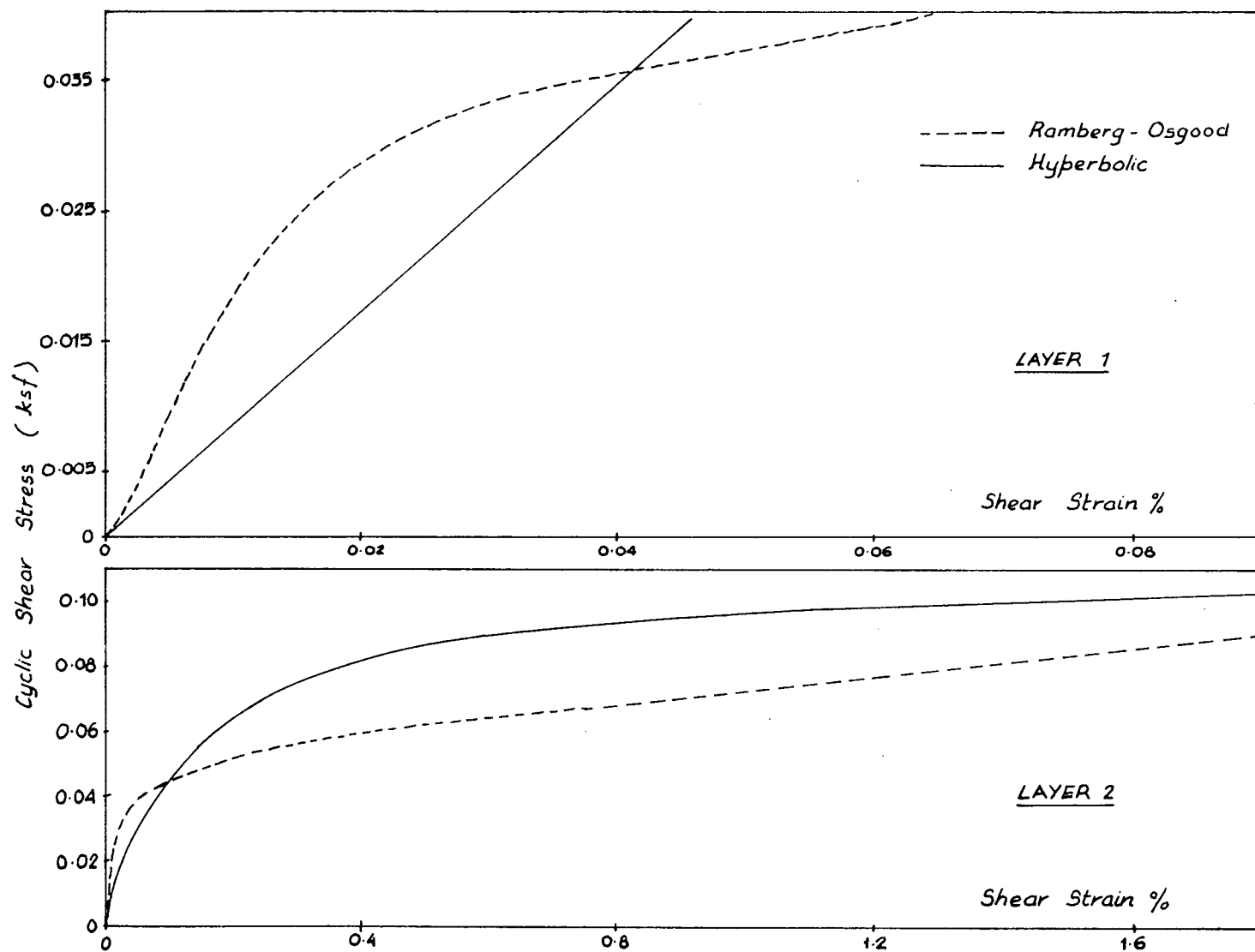   Parameter and Cyclic Strain

Fig.6.6   Stress Strain Curves for the Example Run.
(a) Layers 1 and 2
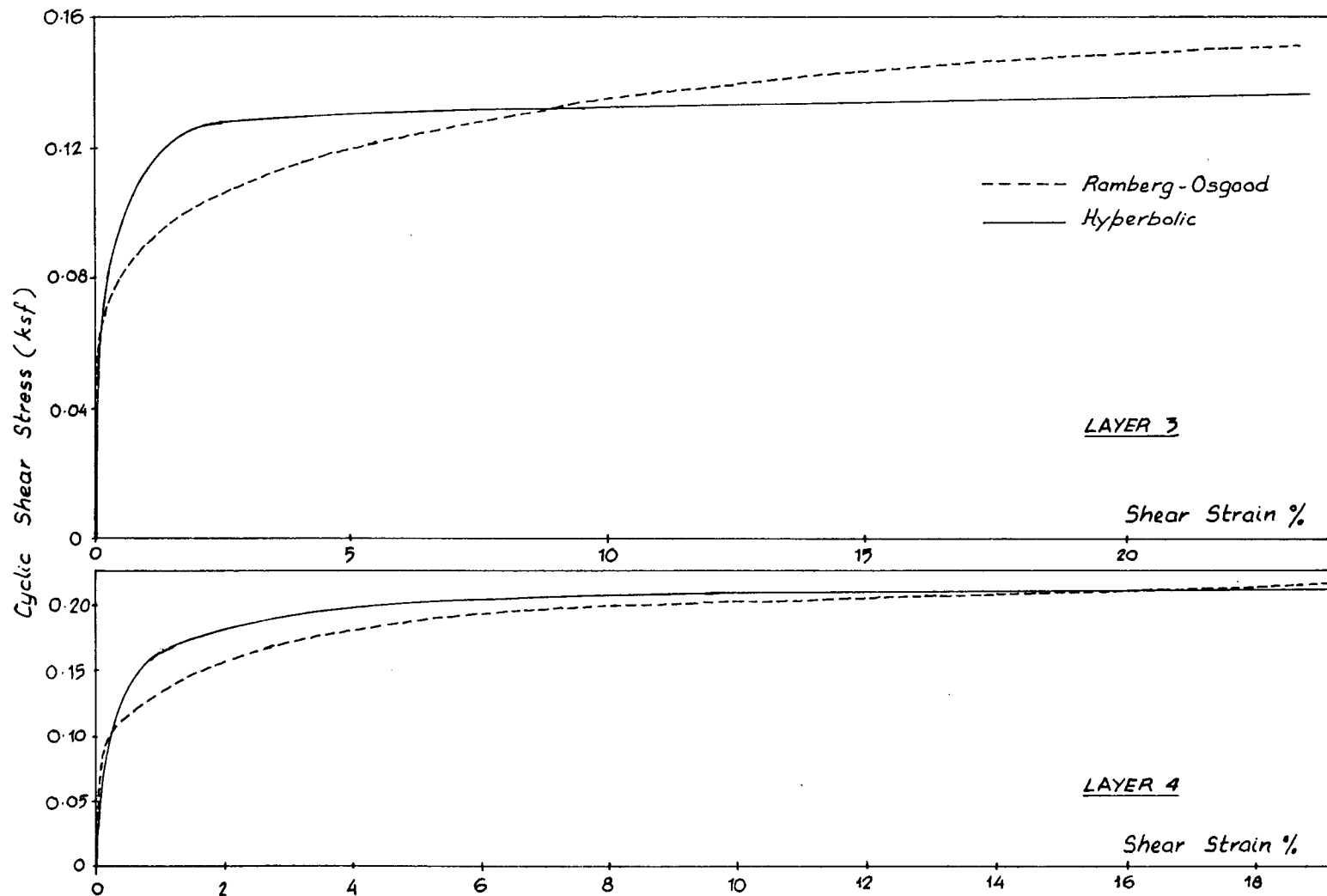
Fig.6.6   Stress Strain Curves for the Example Run.
(b) Layers 3 and 4
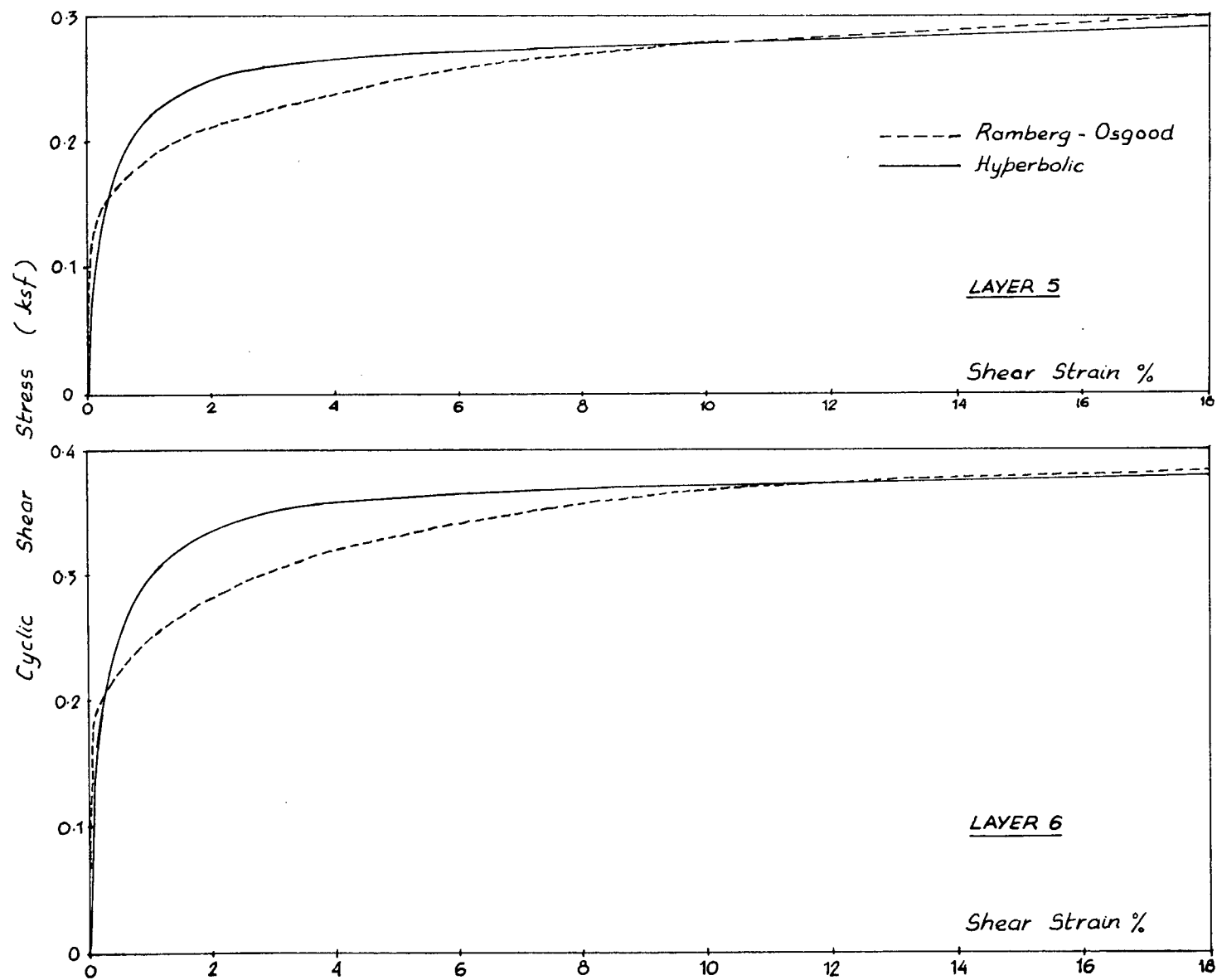
Fig.6.6. Stress Strain Curves for the Example Run.
(c) Layers 5 and 6
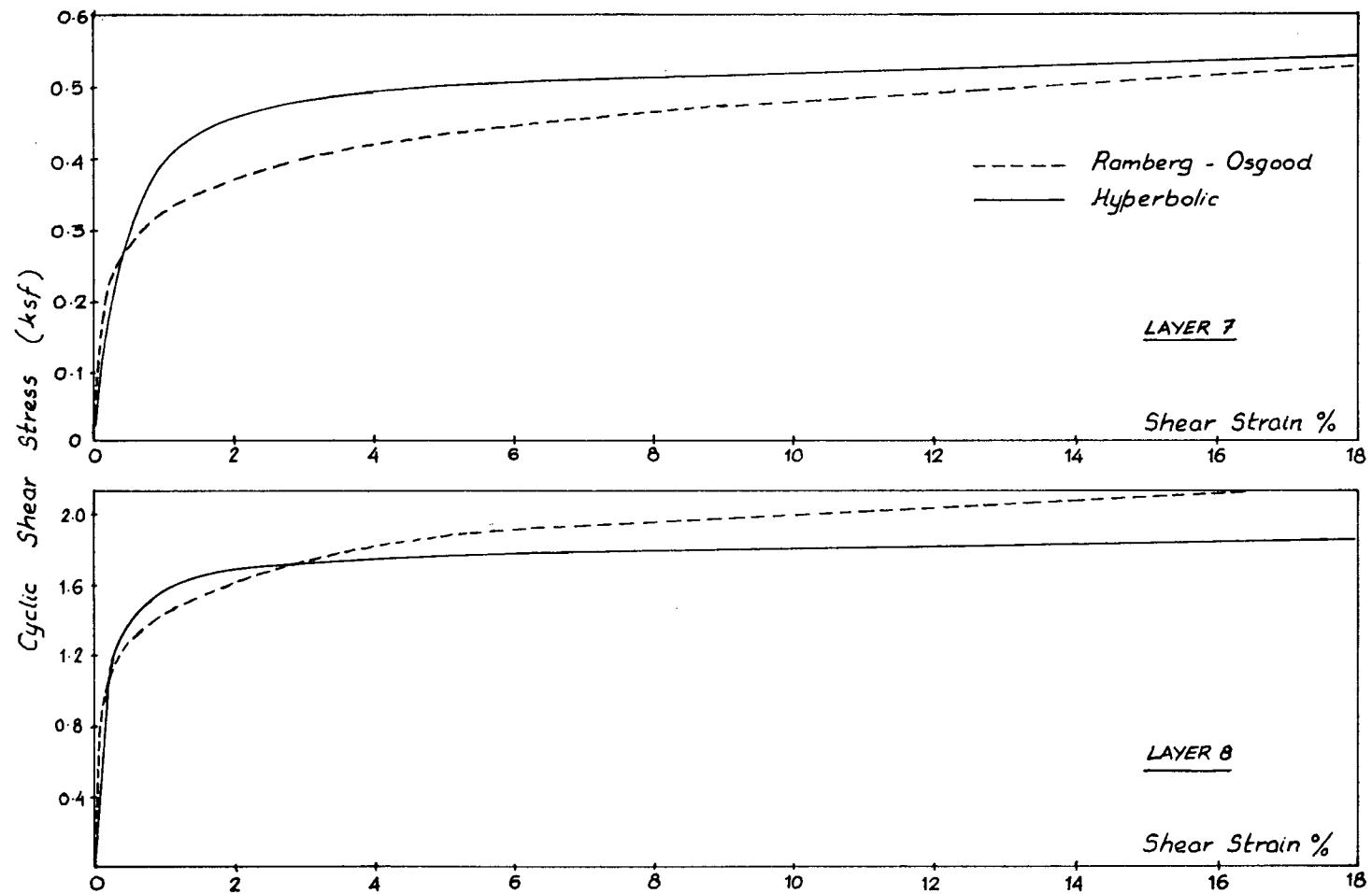
Fig.6.6   Stress Strain Curves for the Example Run.
(d) Layers 7 and 8

reasonably matched in the range of strain levels developed.

6.3 Conclusions.

By comparing the theories and the assumptions made, it was decided in Chapter 5 that, modified Sarma's method is the most suitable rigid body analysis procedure to use in practice. This conclusion is verified to a certain extent by comparing the results of rigid body analysis methods with those of more complex, non-linear effective stress programme DONAL-2. However, it is still a problem to decide upon the value of A parameter to use in a particular problem. In the example problems presented herein, the pore pressure ratios obtained in the two types of analysis were similar. This justifies the values of pore pressure parameters used in these problems.

Comparison between the two non-linear computer programmes, DONAL-2 and DCHARMS is satisfactory. The slightly higher response in DONAL-2 may be due to the difference in the stress strain relation. Ramberg-Osgood curve shows a considerable slope even at very high strain levels. Hyperbolic relation, on the other hand, is asymptotic to the ultimate shear stress, at higher strains. Further and final conclusions are included in Chapter 7.

CHAPTER 7

SUMMARY AND CONCLUSIONS.

7.1 Summary.

The occurence of seafloor slides causing severe
loading conditions on the offshore structures is a major
concern in the oil industry. These slides are caused either by
wave action or by the inertia forces developed by earthquakes.
Critical attention to the latter was given in preceeding pages
of this thesis.

It has long been recognised that the vulnerability of
earth slopes to earthquake induced forces should be assesed by
the displacements of the slope surface under such forces and
not by the usual factor of safety. Calculation of the
displacements of an earth slope under ground shaking can be
carried out in two different methods.

(1) Pseudo-static method of analysis.

(2) Computer programmes based on one dimensional

wave   propagation theory

Rigid body response analysis, one of the pseudo-

static types, was the major interest of several researchers after Newmark's classic paper (1965) on earthquake stability of Dams and Embankments. This, in spite of its simplicity and ease of use, suffers from lack of accuracy. More complex, non-linear computer programmes, on the other hand, require more accurate data and some are costly to use. Hence, it was necessary to find out whether any of the available rigid body analysis methods can be modified to get a reasonably accurate estimate on offshore slope displacements under earthquake loading conditions.

Seed and Goodman's (1966) method was considered first but was not in the case of dry slopes. Sarma's (1975) method was modified for offshore slopes and compared with Pender's (1982) method on a theoretical basis. Comparing the assumptions involved and the calculated critical accelerations, it was decided to leave away Pender's method and to carry out further comparisons with modified Sarma's method.

However, a computer programme was developed to carry out the rigid body type analysis by any of the three methods discussed in the preceeding paragraph. Seed and Goodman's and Modified Sarma's methods were compared to non-linear effective stress analysis procedures by calculating displacements in example slopes. Slopes composed of soils of frictional, cohesive and both frictional and cohesive were selected as example problems. Finally, a recently developed computer programme DCHARMS, was compared with DONAL-2 by analysing a

clay slope. A fairly good agreement was seen between the results despite the differences between the programmes.

7.2 Conclusions.

The work, which has been presented in this thesis leads to following conclusions.

(a) A simple, yet reliable method of calculating offshore slope deformations under earthquake loading is in need at the present time.

(b) Pender's (1982) model does not satisfy some of the necessary requirements of displacement calculation as it results in some unacceptable deformation patterns.

(c) Sarma's method, when modified for offshore applications, gives reasonably agreeing residual deformations under a given earthquake input. But the selection of pore pressure parameter A to use in a given problem is still very difficult.

(d) The rigid body methods are compared only against a complex computer programme. Verification is required either by model testing or by a comparison with field data.

(e) An interesting agreement is seen between DONAL-2 and DCHARMS. Hence, the use of true non-linear coputer programmes in offshore application is

verified to a great extent by this study.

REFERENCES.

1. AMBRASEYS, N. N., 1960, "The Seismic Stability of Earth Dams", Proc., 2nd World Conference on Earthquake Engineering, Japan, Vol.2, 1960.

2. AMBRASEYS, N. N., 1973, "Dynamics and Response of Foundation Materials in Epicentral Regions of Strong Earthquakes", Proc., 5th World Conference on Earthquake Engineering, Rome, 1973.

3. AMBRASEYS, N. N. and SARMA, S. K., 1967, "The Response of Earth Dams to Strong Earthquakes", Geotechnique 17, No.3, pp 181-213, 1967.

4. BYRNE, P. M., 1979, "Elastic Viscoplastic Response of Earth Structures to Earthquake Motion", Thesis Submitted for Partial Fulfillment of the Requirements for the Degree of Doctor of Philosophy in the Department of Civil Engineering, University of British Columbia, Vancouver, B. C., Canada. 1979.

5. De JOSSELIN de JONG, G., 1971, "The Double Sliding Free Rotating Model for Granular Assembles", Discussion, Geotechnique 21, pp 156 - 163, 1971.

6. FINN, W. D. L., 1966, "Earthquake Stability of Cohesive Slopes", Journal of Soil Mechanics and Foundation Division, ASCE, Vol.92, No SM 1, 1966

7. FINN, W. D. L., 1980, "Dynamic Analysis of Soil Structures", CE 581 Lecture Notes, University of British Columbia, 1981/1982.

8. FINN, W. D. L., 1983, "Analysis of Cumulative Deformations Under Cyclic Loading", Invited Challenge Contributed to National Science Foundation Workshop on Expected Research in Soil Engineering, Blacksberg, Verginia, USA, Aug 22 - 24, 1983.

9. FINN, W. D. L. and BYRNE, P. M., 1969, "Seismic Response of Slopes", Proc., 7th International Conference on Soil Mechanics and Foundation Engineering, Vol. 2, Mexico, 1979.

10. FINN, W. D. L., BYRNE, P. M. and MARTIN, G. R., 1976, "Seismic Responce and Liquefaction of Sands", Journal of Geotechnical Engineering Division, ASCE, No.678, Proc. paper 12323, pp 841-856, 1976.

11. FINN, W. D. L., MARTIN, G. R. and LEE, MICHAEL K. W., 1978, "Comparison of Dynamic Analysis of Saturated Sands", Proc., ASCE Geotechnical Engineering Division Speciality Conference, Pasadena, California, pp 472-491, June 19-21, 1978.

12. FINN, W. D. L. and MILLER, R. I. S., 1973, "Dynamic Analysis of Plane Non-Linear Earth Structures", 5th World Conference in Earthquake Engineering, Rome, Session 1D, Paper 42, pp 360 - 367.

13. GOODMAN, R. E. and SEED, H. B., 1966, "Earthquake induced Displacements in Sand Embankments", Journal of Soil Mechanics and Foundation Division, ASCE, Vol.92, No SM 2, pp 125 - 146, March 1966.

14. HATANAKA, M., "Fundamental Considerations on the Earthquake Resistant Properties of The Earth Dam", Bulletin No. 11, Disaster Prevention Research Institute, Kyoto University, Japan, Dec. 1955.

15. IAI, SUSUMU and FINN, W. D. L., 1978, "DONAL-2, A Computer Program for Dynamic One Dimensional Analysis of Slope Layers with Energy Transmitting Boundary", Soil Dynamics Group, University of British Columbia, Vancouver, B. C., Canada, February 1982.

16. IDRISS, I. M., DOBRY, R., DOYCE, E. H. and SINGH, R. D., 1976, "Behaviour of Soft Clays Under Earthquake Loading Conditions", OTC 2671, Offshore Technology Conference, 1976.

17. KRISHNA, J., 1962, "Earthquake Resistant Design of Earth Dams", Proc., Earthquake Symposium held at Roorkee University, Roorkee, India, November 1962.

18. LEE, MICHAEL K. W. and FINN, W. D. L., 1978, "DESRA 2- A Computer Program for the Dynamic Effective Stress Response Analysis of Soil Deposits with Energy Transmitting Boundary including Assesment of Liquefaction Potential", Soil Mechanics No. 38, Department of Civil Engineering, University of British Columbia, Vancouver, B. C., Canada, June 1978.

19. MAKDISI, F. I., and SEED, H. B., 1978, "Simplified Procedure for Estimating Dam and Embankment Earthquake Induced Deformations", Journal of Geotechnical Engineering Division, ASCE, Proc. paper 13898, pp 849-868, July 1978,

20. MONONOBE, M., TAKATA, A. and MATUMURA, M., 1966, "Seismic Stability of the Earth Dam", Proc., 2nd International Congress on Large Dams, held at Washington, D. C., Vol.4, 1966.

21. MORIWAKI, Y., IDRISS, I. M. and DOYLE, E. H., 1982, "Earthquake Induced Deformations of Soft Clay Slopes", Journal of The Geotechnical Engineering Division, ASCE, No. GT 11, November 1982, pp 1475 - 1493

22. National Research Council, U. S. A., 1982, "Earthquake Engineering Research - 1982", Report by Commitee on Earthquake Engineering Research, National Acadamy Press, Washington, D. C., 1982.

23. NEWMARK, N. M., 1965, "Effect of Earthquakes on Dams and Embankments", Geotechnique, Vol.15, No.2, 1965.

24. PENDER, M. J., 1982, "Earthquake Resistant Displacements in Underwater Slopes", Unpublished Report, Soil Dynamics Group, University of British Columbia, Vancouver, B. C., Canada, 1982.

25. RANDOLPH, M. F. and WROTH, C. P., 1981, "Application of the Failure State in Undrained Simple Shear to the Shaft Capacity of Driven Piles", Geotechnique 31, No.1, pp 143 - 157, 1981.

26. RASHID, Y. R., 1961, "Dynamic Response of Earth Dams to Earthquakes", Graduate Student Research Report, University of California, Berkely, California, 1961.

27. SARMA, S. K., 1975, "Seismic Stability of Earth Dams and Embankments", Geotechnique 25, No.4, pp 743-761, 1975.

28. SEED, H. B., 1966, "A Method of Earthquake Resistant Design of Earth Dams", Journal of Soil Mechanics and Foundations Division, ASCE, Vol.92, No. SM 1, January 1966.

29. SEED, H. B., 1967, "Slope Stability During Earthquakes", Proc., Journal of Soil Mechanics and Foundation Division, ASCE, Vol.93, No.SM 4, Proc.paper 5319, pp 299-323, 1967.

30. SEED, H. B., 1979, "Considerations in the Earthquake Resistant Design of Earth and Rockfill Dams", 19th Rankine Lecture, Geotechnique 29, No.3, pp 215 - 263, 1979.

31. SEED, H. B. and GOODMAN, R. E., 1964, "Earthquake Stability of Slopes of Cohesionless Soils", Journal of Soil Mechanics and Foundations Division, ASCE, No. SM 6, pp 43 - 73, November 1964.

32. SEED, H. B. and LEE, K. L., 1966, "Liquefaction of Saturated Sands During Cyclic Loading, Journal of Soil Mechanics and Foundation Division, ASCE, Vol.92, No.SM 6, Proc. paper 4972, pp 105-134, 1966.

33. SEED, H. B. and MARTIN, G. R., 1966, "The Seismic Coefficient in Earth Dam Design", Journal of Soil Mechanics and Foundation Division, ASCE, Vol.92, No.SM 3, Proc. paper 4824, pp 25-58, May 1966.

APPENDIX.

Documentation of the Computer Program OSSA

1.   PROGRAM IDENTIFICATION AND ABSTRACT

1.1   Program Name   OSSA

1.2   Program Title   Offshore Slope Analysis

1.3   Date   May 1982

1.4   Authors   Sarath B. S. Abayakoon and

                                      W. D. Liam Finn,

                                      Soil Dynamics Group,

                                      2075, Wesbrook Mall,

                                      University of British

                                      Columbia,

                                      Vancouver, B. C.,

                                      Canada.

1.5   Computer Requirements

        The computer programme is written in Fortran IV and
has been developed and test run through the use of an AMDHAL
460 computer.

1.6 Abstract

This programme is written to analyse the stability of slopes, either on shore or offshore, shaken by horizontal accelerations. The programme can carry out displacement calculations via three different methods, based on simple rigid body type analyses.

2. DESCRIPTION OF INPUT CARDS

Analysis can be carried out in two different methods. In the first method, a constant shear strength for the soil is assumed throughout the analysis. In the second method, user can allow the shear strength to drop down to zero after the initiation of displacement. The type of analysis to be carried out by the computer programme is controlled by specifying the value of IOPTI as described in card 2.2. Key input variables are explained in the order of input cards as follows.

2.1 Title card (20A4)

Cols. 1-80   TITLE   Eighty characters to describe the title

2.2 Analysis and output control and soil and slope properties (3I4,7F7.4)

Cols. 1-4   IOPTI   Analysis control number

= 0, if shear strength drops to zero after the first displacement

= 1, if shear strength is fully

mobilized all the time

Cols. 5-8   ITOTA   Output control number

= 0, if only the final displacement is
      to be printed.

= 1, if values at specified time
      intervals are to be printed.

Cols. 9-12   IACCN   Negative critical acceleration control
                      number

= 0, if negative critical acceleration
      is higher than positive critical
      acceleration.

= 1, if negative critical acceleration
      is numerically equal to positive
      critical acceleration.

= 2, if negative critical acceleration
      is very high resulting in no
      displacements in the negative
      direction.

Cols. 13-19   SKEMA   Skempton's A parameter

Cols. 20-26   SKEMB   Skempton's B parameter

Cols. 27-33   PHI   Friction angle in degrees.

Cols. 34-40   RO   Mass density of soil.

Cols. 41-47   ROW   = 0.0, if the slope is not submerged

= Mass density of water, if the slope is
      submerged (in the same units as RO)

Cols. 48-54   G   Gravitational acceleration in user's
                       units.

```
Cols. 55-61    SLOPE    Slope angle in degrees.
Cols. 62-68    TI       Time interval at which values are to be
                        printed.
```

2.3 Cohesion and Depth of sliding   (2F10.4)

```
Cols. 1-10     SI       Cohesion intercept (in user's units)
Cols. 11-20    DI       Depth of sliding surface (in user's
                        units).
```

2.4 Initial Conditions and Parameters of Acceleration Record
     (5F9.7,I4)

```
Cols. 1-9      DISP     Initial displacement
Cols. 10-18    VELO     Initial velocity
Cols. 19-27    ACCN     Initial acceleration
Cols. 28-36    DT       Time interval (in seconds) of the input
                        acceleration record.
Cols. 37-45    SCALE    Scale factor to be used to bring the
                        maximum acceleration of earthquake
                        record to a desired maximum acceleration
                        (in gravity units). e.g., If it is
                        necessary to bring 10.0 ft/s  down to
                        0.1g, SCALE = 0.01.
Cols. 46-54    N        Number of earthquake acceleration values
                        per card.
```

2.5 Format Card   (20A4)

```
Cols. 1-80     FMT      A format statement, e.g.,(10F8.4)
```

instructing the computer to read the
acceleration values.

2.6 Earthquake Record Input Data Cards   (FMT)

Earthquake acceleration values measured in time
interval, DT. Any number of cards can be used. N number of
acceleration values per card.

***** END OF INPUT DATA *****